Nonconforming time discretization based on Robin transmission conditions for the Stokes-Darcy system

Thi-Thao-Phuong Hoang[a,1], Hemanta Kunwar[b,2], Hyesuk Lee[c,2,*]

[a]*Department of Mathematics and Statistics, Auburn University, Auburn, AL 36849-0001*
[b]*School of Mathematical and Statistical Sciences, Clemson University, Clemson, SC 29634-0975*
[c]*School of Mathematical and Statistical Sciences, Clemson University, Clemson, SC 29634-0975*

Abstract

We consider a space-time domain decomposition method based on Schwarz waveform relaxation (SWR) for the time-dependent Stokes-Darcy system. The coupled system is formulated as a time-dependent interface problem based on Robin-Robin transmission conditions, for which the decoupling SWR algorithm is proposed and proved for the convergence. In this approach, the Stokes and Darcy problems are solved independently and globally in time, thus allowing the use of different time steps for the local problems. Numerical tests are presented for both non-physical and physical problems with various mesh sizes and time step sizes to illustrate the accuracy and efficiency of the proposed method.

Keywords: Stokes-Darcy system, Domain decomposition, Robin-Robin conditions, Schwarz waveform relaxation, Robin parameters, Local time-stepping

1. Introduction

In many engineering and biological applications, the Stokes-Darcy system is used to model the interaction of fluid flow with porous media flow, where

*Corresponding author
Email addresses: tzh0059@auburn.edu (Thi-Thao-Phuong Hoang), hkunwar@g.clemson.edu (Hemanta Kunwar), hklee@clemson.edu (Hyesuk Lee)
[1]Partially supported by the NSF under grant number DMS-1912626.
[2]Partially supported by the NSF under grant number DMS-1818842.

the Stokes equations represent an incompressible fluid and the Darcy equations represent a flow through a porous medium. Such models are often considered for studying groundwater flows problems [17, 19], filtration [48], flows in a vuggy porous medium [1, 2], and also for understanding impact of stream pollution in water supply [42] and other issues involving water contamination. In health sciences, the Stokes and Darcy equations are used to model filtrations involved in the pharmaceutical and chemical fields [36], biofluid-organ interactions or the movement of blood within vessels [16].

A variety of solution algorithms have been proposed for the numerical approximation of the Stokes-Darcy system. The Stokes-Darcy system is studied as a coupled monolithic system in [1, 2, 36, 51], and some decoupled algorithms are investigated in [6, 9, 10, 26, 27, 39, 49, 53]. A monolithic approach is computationally complex as it requires solving a large linear system; therefore, one often needs the development of efficient and appropriate preconditioners for the discretized linear system. Fully coupled approaches include the use of new finite element spaces [1, 2], Lagrange multiplier spaces [3, 24, 33, 42], or fully discontinuous approximations [50] to approximate the coupled Stokes-Darcy system. Decoupling approaches allow operations on a smaller system of linear equations for each subsystem. However, for such methods, difficulties arise in how to iterate between the two subsystems. Most decoupling strategies employ domain decomposition (DD) techniques to allow the use of optimized algorithms for the Stokes and Darcy subproblems. The mortar space methods are considered in [6, 26, 27, 32], where unmatched meshes on the interface and subdomains are used. Optimization-based DD methods are introduced in [23, 49], the two grid approaches are studied in [9, 45], and the boundary integral method are considered in [8, 54]. In [10, 15] DD methods using Robin-Robin conditions are discussed for the Stokes equations coupled with the Darcy equation in the primal form. There, iterative algorithms are analyzed for convergence and numerically tested with various Robin parameters. More DD works using Robin-Robin conditions for the stationary Stokes-Darcy system can be found in [18, 20, 31], where the decoupling schemes are based on the optimized Schwarz method. The non-

stationary Stokes-Darcy problem is studied using the Crank–Nicolson method in [14]. Non-iterative decoupled marching schemes obtained by lagging the interface coupling terms are investigated in [46, 43]; extensions to the case with different subdomain time steps are analyzed in [53, 52]. Parallel, non-iterative, multi-physics DD methods with Robin conditions are proposed to solve the coupled time-dependent Stokes-Darcy system in [11, 35]. In [47], a non-iterative Robin-Robin domain decomposition method is analyzed for the time-dependent Navier-Stokes-Darcy model with Beavers-Joseph interface condition and defective boundary condition.

In classical DD approaches for time-dependent problems, model equations are discretized in time first, and then DD methods are used at each time step. A uniform time step is usually considered in such approaches. Since the time scales in the Stokes domain and Darcy domain could be largely different, it is inefficient to use a uniform time step throughout the entire time domain. Another approach used in some recent works for time-dependent problems is based on global-in-time or space-time DD methods in which iterative algorithms are directly applied to the evolutionary problem. Consequently, each time-dependent subdomain problem is solved independently, leading to an efficient way to simulate time-dependent phenomena as different time discretization schemes and time step sizes can be used in the subsystems. In [39], we developed a global-in-time DD method based on the physical transmission conditions for the nonlinear Stokes-Darcy coupling. A time-dependent Steklov-Poincaré type operator was constructed, and non-matching time grids were implemented with the use of L^2 projection functions to exchange data on the space-time interface between different time grids.

In this work, we study another global-in-time DD method, namely the Schwarz waveform relaxation (SWR) method with Robin transmission conditions, for the mixed formulation of the non-stationary Stokes-Darcy system using nonconforming time discretization. It should be noted that the convergence of the classical Schwarz waveform relaxation algorithm can be improved by optimizing the coefficients associated with the transmission conditions used

in exchanging space-time boundary data between subdomains, and such an approach is called optimized Schwarz waveform relaxation (OSWR). This method was introduced for parabolic and hyperbolic problems in [29], and it was extended to various problems such as advection-reaction-diffusion problems [44], the compressible Euler equations [22] and the full Maxwell system [21]. It has been implemented in various other works (see, e.g., [5, 7, 29, 30, 37, 44]). For evolutionary multiphysics problems, the choice of Robin coefficients involved in the SWR algorithm is still an open question, and we shall discuss how Robin coefficients affect the accuracy of numerical solutions in our numerical experiments.

This paper is organized as follows. In Section 2, we introduce the model problem, the linear Stokes–Darcy system. In Section 3, we derive a space-time interface problem based on Robin transmission conditions and present the SWR algorithm and its convergence analysis. The semi-discrete, nonconforming in time, SWR algorithm and its convergence are discussed in Section 4. Numerical tests are performed for non-physical and physical problems, and the results are presented in Section 5.

2. Model Equations

Suppose the domain under consideration is made up of two regions $\Omega_f, \Omega_p \subset \mathbb{R}^d$, $d = 2, 3$, separated by the common interface $\Gamma = \partial\Omega_f \cap \partial\Omega_p$. The first region Ω_f is occupied by a free fluid flow and has the Lipschitz boundary $\partial\Omega_f = \Gamma_D^f \cup \Gamma$ and the second region Ω_p is occupied by a saturated porous structure with the Lipschitz boundary $\partial\Omega_p = \Gamma_N^p \cup \Gamma$ (see Figure 1). For the fluid flow in Ω_f we consider the Stokes equations with no-slip boundary condition on Γ_D^f:

$$\frac{\partial \mathbf{u}_f}{\partial t} - 2\nu_f \nabla \cdot D(\mathbf{u}_f) + \nabla p_f = \mathbf{f}_f \quad \text{in } \Omega_f \times (0,T)\,, \tag{2.1}$$

$$\nabla \cdot \mathbf{u}_f = 0 \quad \text{in } \Omega_f \times (0,T)\,, \tag{2.2}$$

$$\mathbf{u}_f = 0 \quad \text{on } \Gamma_D^f \times (0,T), \tag{2.3}$$

$$\mathbf{u}_f(\cdot,0) = \mathbf{u}_{f0} \quad \text{in } \Omega_f, \tag{2.4}$$

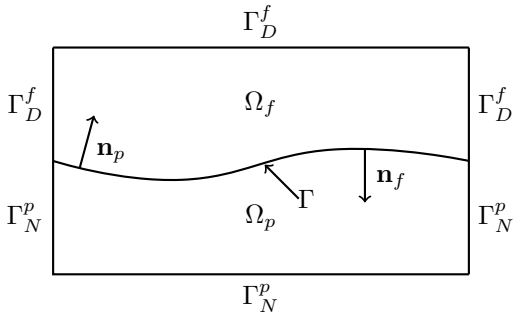

Figure 1: Stokes-Darcy domain

where $\mathbf{u}_f$ denotes the velocity vector, p_f the pressure, ν_f the fluid viscosity, $\mathbf{f}_f$ the body force acting on the fluid and $D(\mathbf{u}_f) := \frac{1}{2}\left(\nabla \mathbf{u}_f + (\nabla \mathbf{u}_f)^T\right)$ the rate of strain tensor. The porous medium flow is represented by the Darcy model with no-flux boundary condition on Γ_N^p:

$$\begin{aligned}
\mu_{eff}\mathbf{K}^{-1}\mathbf{u}_p + \nabla p_p &= 0 \quad \text{in } \Omega_p \times (0,T)\,, && (2.5)\\
\frac{\partial}{\partial t}(s_0 p_p) + \nabla \cdot \mathbf{u}_p &= f_p \quad \text{in } \Omega_p \times (0,T)\,, && (2.6)\\
\mathbf{u}_p \cdot \mathbf{n}_p &= 0 \quad \text{on } \Gamma_N^p \times (0,T), && (2.7)\\
p_p(\cdot,0) &= p_{p0} \quad \text{in } \Omega_p, && (2.8)
\end{aligned}$$

where p_p is the pore pressure, $\mathbf{u}_p$ the Darcy velocity and f_p the source/sink term. The constrained specific storage coefficient is denoted by s_0, μ_{eff} represents the effective fluid viscosity, and $\mathbf{K}$ the permeability tensor of the porous medium. In general, $\mathbf{K}$ is a symmetric positive definite tensor. For simplicity, we assume that $\mu_{eff}\mathbf{K}^{-1}$ is represented by $\nu_p\mathbf{I}$, i.e., $\mu_{eff}\mathbf{K}^{-1} := \nu_p\mathbf{I}$ for some scalar function ν_p.

In order to complete the Stokes-Darcy model, we impose the following interface conditions on $\Gamma \times (0,T)$:

$$\begin{aligned}
\mathbf{u}_f \cdot \mathbf{n}_f + \mathbf{u}_p \cdot \mathbf{n}_p &= 0\,, && (2.9)\\
\mathbf{n}_f \cdot (p_f\mathbf{I} - 2\nu_f D(\mathbf{u}_f)) \cdot \mathbf{n}_f &= p_p\,, && (2.10)\\
\mathbf{n}_f \cdot (p_f\mathbf{I} - 2\nu_f D(\mathbf{u}_f)) \cdot \mathbf{t}_j &= c_{BJS}\mathbf{u}_f \cdot \mathbf{t}_j, j = 1, ..., d-1\,, && (2.11)
\end{aligned}$$

where $\mathbf{n}_f$ and $\mathbf{n}_p$ denote outward unit normal vectors to Ω_f and Ω_p, respectively, $\mathbf{t}_j, j = 1, ..., d-1$ denote the orthogonal set of unit tangent vectors on Γ, and c_{BJS} denotes the resistance parameter in the tangential direction. The interface condition (2.9) enforces the mass conservation across the interface, by enforcing the continuity of the normal velocities, (2.10) enforces the continuity of the normal component of normal stress tensor and (2.11) is the Beavers-Joseph-Saffman condition [40]. These interface conditions suffice to precisely couple the Stokes system (2.1)-(2.4) to the Darcy system (2.5)-(2.8).

We use standard notation for Sobolev spaces, their associated norms and seminorms to define a weak formulation of the problem. For example, for an open domain $\Theta \subset \mathbb{R}^d$, $W^{m,p}(\Theta)$ is the usual Sobolev space with the norm $\|\cdot\|_{m,p,\Theta}$. In case of $p = 2$, the Sobolev space $W^{m,2}(\Theta)$ is denoted by $H^m(\Theta)$ with the norm $\|\cdot\|_{m,\Theta}$. When $m = 0$, $H^m(\Theta)$ coincides with $L^2(\Theta)$. In this case, the inner product and the norm will be denoted by $(\cdot,\cdot)_\Theta$ and $\|\cdot\|_\Theta$, respectively. Moreover, if $\Theta = \Omega_f$ or Ω_p, and the context is clear, Θ will be omitted, i.e., $(\cdot,\cdot) = (\cdot,\cdot)_{\Omega_f}$ or $(\cdot,\cdot)_{\Omega_p}$ for functions defined in Ω_f and Ω_p. Finally, the associated space of vector valued functions will be denoted by a boldface font. Define the following function spaces for $(\mathbf{u}_f, p_f)$ and $(\mathbf{u}_p, p_p)$:

$$
\begin{aligned}
&\mathbf{X}_f := \{\mathbf{v} \in \mathbf{H}^1(\Omega_f) : \ \mathbf{v} = \mathbf{0} \quad \text{on } \Gamma_D^f\},\\
&Q_f := L^2(\Omega_f),\\
&\mathbf{V}_f := \{\mathbf{v}_f \in \mathbf{X}_f : (q_f, \nabla\cdot\mathbf{v}_f) = 0, \forall q_f \in Q_f\},\\
&\widehat{\mathbf{X}}_p := \{\mathbf{v} \in \mathbf{H}^{\mathrm{div}}(\Omega_p) : \mathbf{v}\cdot\mathbf{n}_p = 0 \quad \text{on } \Gamma_N^p\},\\
&\mathbf{X}_p := \{\mathbf{v} \in \widehat{\mathbf{X}}_p : \mathbf{v}\cdot\mathbf{n} \mid_{\partial\Omega_p} \in L^2(\partial\Omega_p)\},\\
&Q_p := L^2(\Omega_p),
\end{aligned}
$$

where $\mathbf{X}_p$ is equipped with the norm

$$\|\mathbf{v}\|^2_{\mathbf{X}_p} := \|\mathbf{v}\|^2_{\mathbf{H}^{\mathrm{div}}(\Omega_p)} + \|\mathbf{v}\cdot\mathbf{n}\|^2_{\partial\Omega_p}.$$

Note that $\mathbf{X}_p$ is a subspace of $\widehat{\mathbf{X}}_p$ with the additional regularity condition. The L^2-regularity of the normal trace of $\mathbf{v} \in \mathbf{X}_p$ is needed for the convergence

proof presented in the next section. The spaces $\mathbf{X}_f$ and Q_f satisfy the inf-sup condition,

$$\inf_{q_f \in Q_f} \sup_{\mathbf{v}_f \in \mathbf{X}_f} \frac{(q_f, \nabla \cdot \mathbf{v}_f)}{\|q_f\| \|\nabla \mathbf{v}_f\|} \geq \beta > 0. \tag{2.12}$$

The dual spaces $\mathbf{X}_f^*$ and $\mathbf{V}_f^*$ are endowed with the following dual norms

$$\|\mathbf{w}\|_{\mathbf{X}_f^*} := \sup_{\mathbf{v}_f \in \mathbf{X}_f} \frac{(\mathbf{w}, \mathbf{v}_f)}{\|\nabla \mathbf{v}_f\|}, \quad \|\mathbf{w}\|_{\mathbf{V}_f^*} := \sup_{v_f \in \mathbf{V}_f} \frac{(\mathbf{w}, \mathbf{v}_f)}{\|\nabla \mathbf{v}_f\|}.$$

These norms are equivalent for functions in $\mathbf{V}_f$ as stated in the following lemma.

Lemma 2.1. *Let $\mathbf{w} \in \mathbf{V}_f$. Then, there exists $C_* > 0$ such that*

$$C_* \|\mathbf{w}\|_{\mathbf{X}_f^*} \leq \|\mathbf{w}\|_{\mathbf{V}_f^*} \leq \|\mathbf{w}\|_{\mathbf{X}_f^*}.$$

Proof. See Lemma 1 in [34]. □

For the variational formulation of the coupled Stokes-Darcy system, we introduce the Lagrange multiplier $\lambda \in L^2(0,T;\Lambda)$, $\Lambda := H_{00}^{1/2}(\Gamma)$ [42], on the interface representing:

$$\lambda := \mathbf{n}_f \cdot (p_f \mathbf{I} - 2\nu_f D(\mathbf{u}_f)) \cdot \mathbf{n}_f = p_p \quad \text{on } \Gamma \times (0,T). \tag{2.13}$$

Let Λ^* be the dual space of Λ. For $\gamma \subset \Gamma$, we use $\langle \cdot, \cdot \rangle_\Gamma$ to denote the duality pairing between Λ and Λ^*. The variational formulation for the Stokes-Darcy system (2.1)-(2.8) satisfying the interface conditions (2.9)-(2.11) reads as: given the initial conditions, find $(\mathbf{u}_f, p_f, \mathbf{u}_p, p_p, \lambda) \in (\mathbf{X}_f, Q_f, \widehat{\mathbf{X}}_p, Q_p, \Lambda)$, for a.e. $t \in (0,T)$, such that

$$\begin{aligned}(\partial_t \mathbf{u}_f, \mathbf{v}_f) + 2\nu_f (D(\mathbf{u}_f), D(\mathbf{v}_f)) - (p_f, \nabla \cdot \mathbf{v}_f) + \sum_{j=1}^{d-1} c_{BJS} (\mathbf{u}_f \cdot \mathbf{t}_j, \mathbf{v}_f \cdot \mathbf{t}_j)_\Gamma \\ = (\mathbf{f}_f, \mathbf{v}_f) + \langle \lambda, \mathbf{v}_f \cdot \mathbf{n}_f \rangle_\Gamma \quad \forall \mathbf{v}_f \in \mathbf{X}_f,\end{aligned} \tag{2.14}$$

$$(q_f, \nabla \cdot \mathbf{u}_f) = 0 \quad \forall q_f \in Q_f, \tag{2.15}$$

$$\nu_p (\mathbf{u}_p, \mathbf{v}_p) - (p_p, \nabla \cdot \mathbf{v}_p) = \langle \lambda, \mathbf{v}_p \cdot \mathbf{n}_p \rangle_\Gamma \quad \forall \mathbf{v}_p \in \widehat{\mathbf{X}}_p, \tag{2.16}$$

$$(q_p, s_0 \, \partial_t p_p) + (q_p, \nabla \cdot \mathbf{u}_p) = (f_p, q_p) \quad \forall q_p \in Q_p, \tag{2.17}$$

$$\langle \mathbf{u}_f \cdot \mathbf{n}_f + \mathbf{u}_p \cdot \mathbf{n}_p, \mu \rangle_\Gamma = 0 \quad \forall \mu \in \Lambda. \tag{2.18}$$

The well-posedness of the stationary Stokes-Darcy model in mixed form can be found in [42] and is assumed to hold similarly for the non-stationary case, i.e. (2.14)-(2.18). For the smooth solutions, the equivalence of the stationary Stokes-Darcy system and the variational formulation is discussed in [24]. The existence and uniqueness of the weak solution to the non-stationary Navier-Stokes-Darcy system with the Beavers-Joseph-Saffman interface condition is studied in [13, 12]; the analysis for the case of Beavers-Joseph interface conditionis done in [11]. In these works, the primal formulation is considered for the Darcy problem, i.e. the velocity and pressure are the unknowns in the fluid flow domain and the pressure is the only unknown in the porous media domain.

3. A global-in-time decoupling scheme

In this section we present a decoupling scheme for the Stokes-Darcy system based on global-in-time domain decomposition. We first rewrite the physical transmission conditions as equivalent Robin conditions and derive the associated space-time interface problem with two interface variables in Subsection 3.1. Such an interface problem is solved iteratively, using Jacobi iterations or GMRES. The former choice is equivalent to the SWR algorithm, which is presented and analyzed in Subsection 3.2.

3.1. Robin transmission conditions and the space-time interface problem

For the Robin transmission conditions on Γ, let α_f and α_p be positive parameters. Combining (2.9) and (2.10) linearly with coefficients $(-\alpha_f, 1)$ and $(\alpha_p, 1)$, we obtain the following two-sided Robin interface conditions on Γ [18]:

$$\mathbf{n}_f \cdot (p_f \mathbf{I} - 2\nu_f D(\mathbf{u}_f)) \cdot \mathbf{n}_f - \alpha_f \mathbf{u}_f \cdot \mathbf{n}_f = p_p + \alpha_f \mathbf{u}_p \cdot \mathbf{n}_p \quad \text{on } \Gamma \times (0,T)\,, \tag{3.1}$$

$$p_p - \alpha_p \mathbf{u}_p \cdot \mathbf{n}_p = \mathbf{n}_f \cdot (p_f \mathbf{I} - 2\nu_f D(\mathbf{u}_f)) \cdot \mathbf{n}_f + \alpha_p \mathbf{u}_f \cdot \mathbf{n}_f \quad \text{on } \Gamma \times (0,T). \tag{3.2}$$

If we let $g_f \in L^2(\Gamma)$ be a Robin condition for the Stokes equations with the parameter $\alpha_f > 0$ as in the left hand side of (3.1), the corresponding weak

formulation is given as follows: find $(\mathbf{u}_f, p_f) \in (\mathbf{X}_f, Q_f)$, for a.e. $t \in (0,T)$, such that

$$(\partial_t \mathbf{u}_f, \mathbf{v}_f) + 2\nu_f(D(\mathbf{u}_f), D(\mathbf{v}_f)) - (p_f, \nabla\cdot\mathbf{v}_f) + \sum_{j=1}^{d-1} c_{BJS}(\mathbf{u}_f\cdot\mathbf{t}_j, \mathbf{v}_f\cdot\mathbf{t}_j)_\Gamma$$
$$+\alpha_f(\mathbf{u}_f\cdot\mathbf{n}_f, \mathbf{v}_f\cdot\mathbf{n}_f)_\Gamma = (\mathbf{f}_f, \mathbf{v}_f) - (g_f, \mathbf{v}_f\cdot\mathbf{n}_f)_\Gamma \quad \forall \mathbf{v}_f \in \mathbf{X}_f\,, \tag{3.3}$$

$$(q_f, \nabla\cdot\mathbf{u}_f) = 0 \quad \forall q_f \in Q_f\,, \tag{3.4}$$

$$(\mathbf{u}_f(\cdot,0), \mathbf{v}_f) = (\mathbf{u}_{f0}, \mathbf{v}_f) \quad \forall \mathbf{v}_f \in \mathbf{X}_f\,. \tag{3.5}$$

Similarly, considering $g_p \in L^2(\Gamma)$ as a Robin condition for the Darcy system with the parameter $\alpha_p > 0$ as in the left hand side of (3.2), we have the weak formulation given by: find $(\mathbf{u}_p, p_p) \in (\mathbf{X}_p, Q_p)$, for a.e. $t \in (0,T)$ satisfying

$$\nu_p(\mathbf{u}_p, \mathbf{v}_p) - (p_p, \nabla\cdot\mathbf{v}_p) + \alpha_p(\mathbf{u}_p\cdot\mathbf{n}_p, \mathbf{v}_p\cdot\mathbf{n}_p)_\Gamma$$
$$= -(g_p, \mathbf{v}_p\cdot\mathbf{n}_p)_\Gamma \quad \forall \mathbf{v}_p \in \mathbf{X}_p\,, \tag{3.6}$$

$$(q_p, s_0\,\partial_t p_p) + (q_p, \nabla\cdot\mathbf{u}_p) = (f_p, q_p) \quad \forall q_p \in Q_p\,, \tag{3.7}$$

$$(p_p(\cdot,0), q_p) = (p_{p0}, q_p) \quad \forall q_p \in Q_p\,. \tag{3.8}$$

Remark 3.1. *From the Robin condition (3.2) with $g_p \in L^2(\Gamma)$ and by the definition of $\mathbf{X}_p$, the trace p_p is in $L^2(\Gamma)$. In fact if the test functions $\mathbf{v}_p$ in (3.6) are chosen to have compact support, then p_p is in $H^1(\Omega_p)$ as shown in [38].*

Denote by $(\mathbf{u}_f, p_f) = \big(\mathbf{u}_f(g_f, \mathbf{f}_f, \mathbf{u}_{f0}), p_f(g_f, \mathbf{f}_f, \mathbf{u}_{f0})\big)$ the solution to the Stokes problem (3.3)-(3.5), and $(\mathbf{u}_p, p_p) = \big(\mathbf{u}_p(g_p, f_p, p_{p0}), p_p(g_p, f_p, p_{p0})\big)$ the solution to the Darcy problem (3.6)-(3.8). To derive the interface problem associated with the Robin conditions (3.1)-(3.2), we first define the interface operator:

$$\mathcal{R} : \Big(L^2(0,T;\, L^2(\Gamma))\Big)^2 \to \Big(L^2(0,T;\, L^2(\Gamma))\Big)^2,$$

such that

$$\mathcal{R}\begin{bmatrix} g_f \\ g_p \end{bmatrix} = \begin{bmatrix} g_p + (\alpha_p + \alpha_f)\left(\mathbf{u}_p(g_p, f_p, p_{p0})\cdot\mathbf{n}_p\right)|_\Gamma \\ g_f + (\alpha_f + \alpha_p)\left(\mathbf{u}_f(g_f, \mathbf{f}_f, \mathbf{u}_{f0})\cdot\mathbf{n}_f\right)|_\Gamma \end{bmatrix}. \tag{3.9}$$

Then the Robin transmission conditions (3.1)-(3.2) are equivalent to the following space-time interface problem for two interface variables:

$$\mathcal{S}_{\mathcal{R}} \begin{bmatrix} g_f \\ g_p \end{bmatrix} = \chi_{\mathcal{R}} \quad \text{on } \Gamma \times (0,T), \tag{3.10}$$

where

$$\mathcal{S}_{\mathcal{R}} \begin{bmatrix} g_f \\ g_p \end{bmatrix} = \begin{bmatrix} g_f \\ g_p \end{bmatrix} - \begin{bmatrix} g_p + (\alpha_p + \alpha_f) \left(\mathbf{u}_p(g_p, 0, 0) \cdot \mathbf{n}_p \right) |_\Gamma \\ g_f + (\alpha_f + \alpha_p) \left(\mathbf{u}_f(g_f, \mathbf{0}, \mathbf{0}) \cdot \mathbf{n}_f \right) |_\Gamma \end{bmatrix},$$

and

$$\chi_{\mathcal{R}} = \begin{bmatrix} (\alpha_p + \alpha_f) \left(\mathbf{u}_p(0, f_p, p_{p0}) \cdot \mathbf{n}_p \right) |_\Gamma \\ (\alpha_f + \alpha_p) \left(\mathbf{u}_f(0, \mathbf{f}_f, \mathbf{u}_{f0}) \cdot \mathbf{n}_f \right) |_\Gamma \end{bmatrix}.$$

The weak form of (3.10) is given by: find $(g_f, g_p) \in \left(L^2(\Gamma)\right)^2$, for a.e. $t \in (0,T)$, such that $\forall \left(\xi_f, \xi_p\right) \in \left(L^2(\Gamma)\right)^2$

$$\int_\Gamma \left(\mathcal{S}_{\mathcal{R}} \begin{bmatrix} g_f \\ g_p \end{bmatrix} \cdot \begin{bmatrix} \xi_f \\ \xi_p \end{bmatrix} \right) d\gamma \; = \; \int_\Gamma \left(\chi_{\mathcal{R}} \cdot \begin{bmatrix} \xi_f \\ \xi_p \end{bmatrix} \right) d\gamma. \tag{3.11}$$

To carry out the convergence analysis of the proposed decoupling scheme, we solve the space-time interface problem (3.10) by Jacobi iterations, which is equivalent to the SWR algorithm and will be presented next. However, for the numerical experiments (cf. Section 5), we will use GMRES to solve the interface problem iteratively for faster convergence.

3.2. Schwarz waveform relaxation (SWR) algorithm

Consider the following SWR algorithm based on Robin transmission conditions: at the kth iteration step we solve

$$\begin{aligned}
\partial_t \mathbf{u}_f^k - \nabla \cdot (2\nu_f D(\mathbf{u}_f^k) - p_f^k \mathbf{I}) &= \mathbf{f}_f \quad \text{in } \Omega_f \times (0,T)\,, && (3.12)\\
\nabla \cdot \mathbf{u}_f^k &= 0 \quad \text{in } \Omega_f \times (0,T)\,, && (3.13)\\
\mathbf{n}_f^k \cdot (p_f^k \mathbf{I} - 2\nu_f D(\mathbf{u}_f^k)) \cdot \mathbf{n}_f - \alpha_f \mathbf{u}_f^k \cdot \mathbf{n}_f &= p_p^{k-1} + \alpha_f \mathbf{u}_p^{k-1} \cdot \mathbf{n}_p \\
&\qquad \text{on } \Gamma \times (0,T)\,, && (3.14)
\end{aligned}$$

for (u_f^k, p_f^k) satisfying the initial and boundary conditions (2.3), (2.4) and the Beavers-Joseph-Saffman condition (2.11), and

$$\begin{aligned} \nu_p \mathbf{u}_p^k + \nabla p_p^k &= 0 \quad \text{in } \Omega_p \times (0,T)\,, && (3.15)\\ s_0 \partial_t p_p^k + \nabla \cdot \mathbf{u}_p^k &= \mathbf{f}_p \quad \text{in } \Omega_p \times (0,T)\,, && (3.16)\\ p_p^k - \alpha_p \mathbf{u}_p^k \cdot \mathbf{n}_p &= \mathbf{n}_f \cdot (p_f^{k-1}\mathbf{I} - 2\nu_f D(\mathbf{u}_f^{k-1}))\mathbf{n}_f + \alpha_p \mathbf{u}_f^{k-1} \cdot \mathbf{n}_f \\ &\qquad \text{on } \Gamma \times (0,T)\,, && (3.17) \end{aligned}$$

for (u_p^k, p_p^k) satisfying (2.7) and (2.8). The weak formulation of this decoupled system is written as follows: at the kth iteration, find $(\mathbf{u}_f^k, p_f^k) \in (\mathbf{X}_f, Q_f)$ and $(\mathbf{u}_p^k, p_p^k) \in (\mathbf{X}_p, Q_p)$, for a.e. $t \in (0,T)$, such that

$$\begin{aligned} &(\partial_t \mathbf{u}_f^k, \mathbf{v}_f) + 2\nu_f (D(\mathbf{u}_f^k), D(\mathbf{v}_f)) - (p_f^k, \nabla \cdot \mathbf{v}_f) + \sum_{j=1}^{d-1} c_{BJS} (\mathbf{u}_f^k \cdot \mathbf{t}_j, \mathbf{v}_f \cdot \mathbf{t}_j)_\Gamma \\ &\quad + \alpha_f (\mathbf{u}_f^k \cdot \mathbf{n}_f, \mathbf{v}_f \cdot \mathbf{n}_f)_\Gamma = (\mathbf{f}_f, \mathbf{v}_f) - (p_p^{k-1} + \alpha_f \mathbf{u}_p^{k-1} \cdot \mathbf{n}_p, \mathbf{v}_f \cdot \mathbf{n}_f)_\Gamma \\ &\qquad \forall \mathbf{v}_f \in \mathbf{X}_f\,, \qquad (3.18)\\ &(q_f, \nabla \cdot \mathbf{u}_f^k) = 0 \quad \forall q_f \in Q_f\,, \qquad (3.19) \end{aligned}$$

and

$$\begin{aligned} &\nu_p (\mathbf{u}_p^k, \mathbf{v}_p) - (p_p^k, \nabla \cdot \mathbf{v}_p^k) + \alpha_p (\mathbf{u}_p^k \cdot \mathbf{n}_p, \mathbf{v}_p \cdot \mathbf{n}_p)_\Gamma \\ &\quad = -(\mathbf{n}_f \cdot (p_f^{k-1}\mathbf{I} - 2\nu_f D(\mathbf{u}_f^{k-1}))\mathbf{n}_f + \alpha_p \mathbf{u}_f^{k-1} \cdot \mathbf{n}_f, \mathbf{v}_p \cdot \mathbf{n}_p)_\Gamma \\ &\qquad \forall \mathbf{v}_p \in \mathbf{X}_p\,, \qquad (3.20)\\ &(q_p, s_0\, \partial_t p_p^k) + (q_p, \nabla \cdot \mathbf{u}_p^k) = (f_p, q_p) \quad \forall q_p \in Q_p\,. \qquad (3.21) \end{aligned}$$

In the next theorem we prove the convergence of the proposed algorithm. The following identities will be used in the proof:

$$\begin{aligned} &(\mathbf{n}_f^k \cdot (p_f^k I - 2\nu_f D(\mathbf{u}_f^k)) \cdot \mathbf{n}_f - \alpha_f \mathbf{u}_f^k \cdot \mathbf{n}_f)^2 \\ &\qquad -(\mathbf{n}_f^k \cdot (p_f^k \mathbf{I} - 2\nu_f D(\mathbf{u}_f^k)) \cdot \mathbf{n}_f + \alpha_p \mathbf{u}_f^k \cdot \mathbf{n}_f)^2 \qquad (3.22)\\ &= -2(\alpha_f + \alpha_p)(\mathbf{u}_f^k \cdot \mathbf{n}_f)(\mathbf{n}_f^k \cdot (p_f^k I - 2\nu_f D(\mathbf{u}_f^k)) \cdot \mathbf{n}_f) + (\alpha_f^2 - \alpha_p^2)(\mathbf{u}_f^k \cdot \mathbf{n}_f)^2, \\ &(p_p^k - \alpha_p \mathbf{u}_p^k \cdot \mathbf{n}_p)^2 - (p_p^k + \alpha_f \mathbf{u}_p^k \cdot \mathbf{n}_p)^2 \\ &\qquad = -2(\alpha_f + \alpha_p) p_p^k (\mathbf{u}_p^k \cdot \mathbf{n}_p) + (\alpha_p^2 - \alpha_f^2)(\mathbf{u}_p^k \cdot \mathbf{n}_p)^2\,. \qquad (3.23) \end{aligned}$$

Theorem 3.1. *Let $\mathbf{f}_f \in \boldsymbol{X}_f^*, f_p \in Q_p$ and let $\alpha_f, \alpha_p \in \mathbb{R}$ be such that $\alpha_p \geq \alpha_f > 0$. If initial values $(\mathbf{u}_f^0, p_f^0, \mathbf{u}_p^0, p_p^0)$ are chosen such that the Robin-Robin conditions (3.14), (3.17) are well-defined in $L^2(\Gamma)$ then the weak formulation (3.18)-(3.21) defines a unique sequence of iterates*

$$(\mathbf{u}_f^k, p_f^k, \mathbf{u}_p^k, p_p^k) \in L^\infty(0,T;\boldsymbol{X}_f) \times L^2(0,T;Q_f) \times L^2(0,T;\boldsymbol{X}_p) \times L^\infty(0,T;Q_p)$$

that converges to the weak solution $(\mathbf{u}_f, p_f, \mathbf{u}_p, p_p)$ of problem (2.14)-(2.18).

Proof. As the equations are linear, for the proof of convergence we take $\mathbf{f}_f = \mathbf{u}_{f0} = \mathbf{0}$ and $f_p = p_{p0} = 0$, and show that the sequence $(\mathbf{u}_f^k, p_f^k, \mathbf{u}_p^k, p_p^k)$ of iterates converges to zero in suitable norms. The uniqueness of the sequence of iterates follows from the well-posedness of non-stationary Stokes-Darcy system.

Choosing $\mathbf{v}_f = \mathbf{u}_f^k$ and $q_f = p_f^k$ in (3.18)-(3.19) and adding two resulting equations yield

$$(\partial_t \mathbf{u}_f^k, \mathbf{u}_f^k) + 2\nu_f \|D(\mathbf{u}_f^k)\|_{\Omega_f}^2 + \sum_{j=1}^{d-1} c_{BJS} \|\mathbf{u}_f^k \cdot \mathbf{t}_j\|_\Gamma^2 + \alpha_f \|\mathbf{u}_f^k \cdot \mathbf{n}_f\|_\Gamma^2 = -(p_p^{k-1} + \alpha_f \mathbf{u}_p^{k-1} \cdot \mathbf{n}_p, \mathbf{u}_f^k \cdot \mathbf{n}_f)_\Gamma.$$

By using the Robin condition (3.14) and (3.22), we obtain

$$\begin{aligned}(\partial_t \mathbf{u}_f^k, \mathbf{u}_f^k) + 2\nu_f \|D(\mathbf{u}_f^k)\|_{\Omega_f}^2 + \sum_{j=1}^{d-1} c_{BJS} \|\mathbf{u}_f^k \cdot \mathbf{t}_j\|_\Gamma^2 \\ + \frac{1}{2(\alpha_f + \alpha_p)} \|\mathbf{n}_f \cdot (p_f^k \mathbf{I} - 2\nu_f D(\mathbf{u}_f^k)) \cdot \mathbf{n}_f + \alpha_p \mathbf{u}_f^k \cdot \mathbf{n}_f\|_\Gamma^2 \\ = \frac{1}{2(\alpha_f + \alpha_p)} \|p_p^{k-1} + \alpha_f \mathbf{u}_p^{k-1} \cdot \mathbf{n}_p\|_\Gamma^2 + \frac{\alpha_p - \alpha_f}{2} \|\mathbf{u}_f^k \cdot \mathbf{n}_f\|_\Gamma^2. \quad (3.24)\end{aligned}$$

In the following, we shall consider the case where α_p is strictly greater than α_f; if $\alpha_p = \alpha_f$, a similar and simpler proof can be obtained (cf. Remark 3.2). We integrate (3.24) over $(0,t)$ for a.e. $t \in (0,T]$, and use the trace theorem, Korn's

inequality and Young's inequality to obtain

$$\begin{aligned}
&\frac{1}{2}\|\mathbf{u}_f^k(t)\|_{\Omega_f}^2 + 2\nu_f\int_0^t \|D(\mathbf{u}_f^k)\|_{\Omega_f}^2\,ds + \sum_{j=1}^{d-1} c_{BJS}\int_0^t \|\mathbf{u}_f^k\cdot\mathbf{t}_j\|_\Gamma^2\,ds \\
&\qquad + \frac{1}{2(\alpha_f+\alpha_p)}\int_0^t \|\mathbf{n}_f\cdot(p_f^k\mathbf{I} - 2\nu_f D(\mathbf{u}_f^k))\cdot\mathbf{n}_f + \alpha_p\mathbf{u}_f^k\cdot\mathbf{n}_f\|_\Gamma^2\,ds \\
&\le \frac{1}{2(\alpha_f+\alpha_p)}\int_0^t \|p_p^{k-1} + \alpha_f\mathbf{u}_p^{k-1}\cdot\mathbf{n}_p\|_\Gamma^2\,ds \\
&\qquad + \overline{C}\int_0^t \|\mathbf{u}_f^k(s)\|_{\Omega_f}\|D(\mathbf{u}_f^k(s))\|_{\Omega_f}\,ds \\
&\le \frac{1}{2(\alpha_f+\alpha_p)}\int_0^t \|p_p^{k-1} + \alpha_f\mathbf{u}_p^{k-1}\cdot\mathbf{n}_p\|_\Gamma^2\,ds \\
&\qquad + \overline{C}\int_0^t \left(\frac{1}{4\epsilon}\|\mathbf{u}_f^k(s)\|_{\Omega_f}^2 + \epsilon\|D(\mathbf{u}_f^k(s))\|_{\Omega_f}^2\right)\,ds,
\end{aligned}$$

for some constant $\overline{C} > 0$ and $\epsilon > 0$. Setting $\epsilon = \nu_f/\overline{C}$, we have

$$\begin{aligned}
&\frac{1}{2}\|\mathbf{u}_f^k(t)\|_{\Omega_f}^2 + \nu_f\int_0^t \|D(\mathbf{u}_f^k)\|_{\Omega_f}^2\,ds + \sum_{j=1}^{d-1} c_{BJS}\int_0^t \|\mathbf{u}_f^k\cdot\mathbf{t}_j\|_\Gamma^2\,ds \\
&\qquad + \frac{1}{2(\alpha_f+\alpha_p)}\int_0^t \|\mathbf{n}_f\cdot(p_f^k\mathbf{I} - 2\nu_f D(\mathbf{u}_f^k))\cdot\mathbf{n}_f + \alpha_p\mathbf{u}_f^k\cdot\mathbf{n}_f\|_\Gamma^2\,ds \\
&\le \frac{1}{2(\alpha_f+\alpha_p)}\int_0^t \|p_p^{k-1} + \alpha_f\mathbf{u}_p^{k-1}\cdot\mathbf{n}_p\|_\Gamma^2\,ds + C\int_0^t \|\mathbf{u}_f^k(s)\|_{\Omega_f}^2\,ds\,, \quad (3.25)
\end{aligned}$$

where $C = \frac{\overline{C}^2}{4\nu_f}$. Similarly, setting $\mathbf{v}_p = \mathbf{u}_p^k, q_p = p_p^k$ in (3.20)-(3.21), adding the resulting equations and using (3.23), we get

$$\begin{aligned}
&\nu_p\|\mathbf{u}_p^k\|_{\Omega_p}^2 + (s_0\,\partial_t p_p^k, p_p^k) + \frac{1}{2(\alpha_f+\alpha_p)}\|p_p^k + \alpha_f\mathbf{u}_p^k\cdot\mathbf{n}_p\|_\Gamma^2 \\
&\qquad\qquad \le \frac{1}{2(\alpha_f+\alpha_p)}\|p_p^k - \alpha_p\mathbf{u}_p^k\cdot\mathbf{n}_p\|_\Gamma^2 - \frac{1}{2}(\alpha_p-\alpha_f)\|\mathbf{u}_p^k\cdot\mathbf{n}_p\|_\Gamma^2\,.
\end{aligned}$$

Let $\gamma := \frac{\alpha_p-\alpha_f}{2} > 0$. We integrate the above inequality over $(0,t)$ for a.e. $t \in (0,T]$ and apply the Robin boundary condition (3.17) to obtain:

$$\begin{aligned}
&\nu_p\int_0^t \|\mathbf{u}_p^k(t)\|_{\Omega_p}^2\,ds + \frac{s_0}{2}\|p_p^k(t)\|_{\Omega_p}^2 + \frac{1}{2(\alpha_f+\alpha_p)}\int_0^t \|p_p^k + \alpha_f\mathbf{u}_p^k\cdot\mathbf{n}_p\|_\Gamma^2\,ds \\
&\qquad + \gamma\int_0^t \|\mathbf{u}_p^k\cdot\mathbf{n}_p\|_\Gamma^2\,ds \\
&\le \frac{1}{2(\alpha_f+\alpha_p)}\int_0^t \|\mathbf{n}_f\cdot(p_f^{k-1}\mathbf{I} - 2\nu_f D(\mathbf{u}_f^{k-1}))\mathbf{n}_f + \alpha_p\mathbf{u}_f^{k-1}.\mathbf{n}_f\|_\Gamma^2\,ds\,. \quad (3.26)
\end{aligned}$$

We add (3.25) and (3.26), and define

$$\begin{aligned} E^k(t) &:= \frac{1}{2}\|\mathbf{u}_f^k(t)\|^2_{\Omega_f} + \nu_f \int_0^t \|D(\mathbf{u}_f^k)\|^2_{\Omega_f}\, ds + \sum_{j=1}^{d-1} c_{BJS} \int_0^t \|\mathbf{u}_f^k \cdot \mathbf{t}_j\|^2_{\Gamma}\, ds \\ &\quad + \nu_p \int_0^t \|\mathbf{u}_p^k(t)\|^2_{\Omega_p}\, ds + \frac{s_0}{2}\|p_p^k(t)\|^2_{\Omega_p} + \gamma \int_0^t \|\mathbf{u}_p^k \cdot \mathbf{n}_p\|^2_{\Gamma}\, ds\,, \\ B^k(t) &:= \frac{1}{2(\alpha_f+\alpha_p)} \int_0^t \|\mathbf{n}_f \cdot (p_f^k \mathbf{I} - 2\nu_f D(\mathbf{u}_f^k))\mathbf{n}_f + \alpha_p \mathbf{u}_f^k.\mathbf{n}_f\|^2_{\Gamma}\, ds \\ &\quad + \frac{1}{2(\alpha_f+\alpha_p)} \int_0^t \|p_p^k + \alpha_f \mathbf{u}_p^k \cdot \mathbf{n}_p\|^2_{\Gamma}\, ds\,. \end{aligned}$$

Then, for all $k > 0$

$$E^k(t) + B^k(t) \le B^{k-1}(t) + C \int_0^t \|\mathbf{u}_f^k(s)\|^2_{\Omega_f}\, ds\,,$$

and summing over the iterates for any given $K > 0$ yields,

$$\sum_{k=1}^{K} E^k(t) \le B^0(t) + C \sum_{k=1}^{K} \int_0^t \|\mathbf{u}_f^k(s)\|^2_{\Omega_f}\, ds, \tag{3.27}$$

where

$$B^0(t) = \frac{1}{2(\alpha_f+\alpha_p)} \int_0^t \int_{\Gamma} g_0\, ds,$$

for $g_0 = (\mathbf{n}_f \cdot (p_f^0 I - 2\nu_f D(\mathbf{u}_f^0))\mathbf{n}_f + \alpha_p \mathbf{u}_f^0.\mathbf{n}_f)^2 + (p_p^0 + \alpha_f \mathbf{u}_p^0 \cdot \mathbf{n}_p)^2$ obtained by the initial guess. Now, from the definition of $E^k(t)$ and (3.27),

$$\frac{1}{2}\sum_{k=1}^{K} \|\mathbf{u}_f^k(t)\|^2_{\Omega_f} \le B^0(t) + C \sum_{k=1}^{K} \int_0^t \|\mathbf{u}_f^k(s)\|^2_{\Omega_f}\, ds.$$

Applying Gronwall's lemma, we obtain

$$\sum_{k=1}^{K} \|\mathbf{u}_f^k(t)\|^2_{\Omega_f} \le 2e^{2CT} B^0(T), \tag{3.28}$$

for any $K > 0$ and a.e. $t \in (0, T)$. The inequality (3.28) implies that $\mathbf{u}_f^k$ tends to 0 in $L^\infty(0, T; \mathbf{L^2}(\Omega_f))$ as $k \to \infty$, and the inequalities (3.27) and (3.28) yield

$$\begin{aligned} &\sum_{k=1}^{K} \left(\nu_f \int_0^t \|D(\mathbf{u}_f^k)\|^2_{\Omega_f}\, ds + \sum_{j=1}^{d-1} c_{BJS} \int_0^t \|\mathbf{u}_f^k \cdot \mathbf{t}_j\|^2_{\Gamma}\, ds + \nu_p \int_0^t \|\mathbf{u}_p^k(t)\|^2_{\Omega_p}\, ds \right. \\ &\left. + \frac{s_0}{2}\|p_p^k(t)\|^2_{\Omega_p} + \gamma \int_0^t \|\mathbf{u}_p^k \cdot \mathbf{n}_p\|^2_{\Gamma}\, ds \right) \le (1 + 2CTe^{2CT}) B^0(T), \end{aligned} \tag{3.29}$$

for any positive integer K. The inequality (3.29) implies that $D(\mathbf{u}_f^k)$, $\mathbf{u}_f^k \cdot \mathbf{t}_j$, $\mathbf{u}_p^k$, p_p^k and $\mathbf{u}_p^k \cdot \mathbf{n}_p$ tend to 0 in $L^2(0,T;\mathbf{L}^2(\Omega_f))$, $L^2(0,T;L^2(\Gamma))$, $L^2(0,T;\mathbf{L}^2(\Omega_p))$, $L^\infty(0,T;L^2(\Omega_p))$ and $L^2(0,T;L^2(\Gamma))$, respectively, as $k \to \infty$.

For the convergence of p_f^k, we follow the technique used in [25]. We isolate the time derivative term in (3.18). Then for all $\mathbf{v}_f \in \mathbf{V}_f$:

$$\begin{aligned}(\partial_t \mathbf{u}_f^k, \mathbf{v}_f) \;=\; & -2\nu_f (D(\mathbf{u}_f^k), D(\mathbf{v}_f)) - \alpha_f (\mathbf{u}_f^k \cdot \mathbf{n}_f, \mathbf{v}_f \cdot \mathbf{n}_f)_\Gamma \\ & - \sum_{j=1}^{d-1} c_{BJS} (\mathbf{u}_f^k \cdot \mathbf{t}_j, \mathbf{v}_f \cdot \mathbf{t}_j)_\Gamma - (p_p^{k-1} + \alpha_f \mathbf{u}_p^{k-1} \cdot \mathbf{n}_p, \mathbf{v}_f \cdot \mathbf{n}_f)_\Gamma \end{aligned} \tag{3.30}$$

For the bounds of right-hand side terms in (3.30) we use Cauchy-Schwarz inequality, the trace theorem, Korn's inequality and Poincaré-Friedrichs inequality, divide both sides by $\left\|\nabla \mathbf{v}_f\right\|_{\Omega_f}$ and take supremum over $\mathbf{v}_f \in \mathbf{V}_f$. Then, for some constants $C_1, C_2, C_3, C_4 > 0$,

$$\begin{aligned}\|\partial_t \mathbf{u}_f^k\|_{\mathbf{V}_f^*} \;\leq\; & 2\nu_f C_1 \|D(\mathbf{u}_f^k)\|_{\Omega_f} + C_2 \|D(\mathbf{u}_f^k)\|_{\Omega_f}^{1/2} \|\mathbf{u}_f^k\|_{\Omega_f}^{1/2} \\ & + \sum_{j=1}^{d-1} c_{BJS} C_3 \|\mathbf{u}_f^k \cdot \mathbf{t}_j\|_\Gamma + C_4 \|p_p^{k-1} + \alpha_f \mathbf{u}_p^{k-1} \cdot \mathbf{n}_p\|_\Gamma \\ \leq\; & \frac{C_2}{2} \|\mathbf{u}_f^k\|_{\Omega_f} + \left(2\nu_f C_1 + \frac{C_2}{2}\right) \|D(\mathbf{u}_f^k)\|_{\Omega_f} + \sum_{j=1}^{d-1} c_{BJS} C_3 \|\mathbf{u}_f^k \cdot \mathbf{t}_j\|_\Gamma \\ & + C_4 \|p_p^{k-1}\|_\Gamma + \alpha_f C_4 \|\mathbf{u}_p^{k-1} \cdot \mathbf{n}_p\|_\Gamma \,. \end{aligned}$$

Setting $\widehat{C} = \max\{\frac{C_2}{2}, (2\nu_f C_1 + \frac{C_2}{2}), c_{BJS} C_3, C_4, \alpha_f C_4\}$, we have

$$\|\partial_t \mathbf{u}_f^k\|_{\mathbf{V}_f^*} \leq \widehat{C}\big(\|\mathbf{u}_f^k\|_{\Omega_f} + \|D(\mathbf{u}_f^k)\|_{\Omega_f} + \sum_{j=1}^{d-1} \|\mathbf{u}_f^k \cdot \mathbf{t}_j\|_\Gamma + \|p_p^{k-1}\|_\Gamma + \|\mathbf{u}_p^{k-1} \cdot \mathbf{n}_p\|_\Gamma \big) \,.$$

Lemma 2.1 then implies

$$\|\partial_t \mathbf{u}_f^k\|_{\mathbf{X}_f^*} \leq C_*^{-1} \widehat{C} (\|\mathbf{u}_f^k\|_{\Omega_f} + \|D(\mathbf{u}_f^k)\|_{\Omega_f} + \sum_{j=1}^{d-1} \|\mathbf{u}_f^k \cdot \mathbf{t}_j\|_\Gamma + \|p_p^{k-1}\|_\Gamma + \|\mathbf{u}_p^{k-1} \cdot \mathbf{n}_p\|_\Gamma) \,. \tag{3.31}$$

Now consider (3.18) with $\mathbf{v}_f \in \mathbf{X}_f$. We isolate pressure term, divide by $\|\nabla \mathbf{v}_f\|$, take supremum over $\mathbf{v}_f \in \mathbf{X}_f$ and use the inf-sup condition (2.12) and the

estimate (3.31). Then, for some $\beta > 0$,

$$\beta\|p_f^k\|_{\Omega_f} \le (1 + C_*^{-1}\widehat{C})(\|\mathbf{u}_f^k\|_{\Omega_f} + \|D(\mathbf{u}_f^k)\|_{\Omega_f} + \sum_{j=1}^{d-1} \|\mathbf{u}_f^k \cdot \mathbf{t}_j\|_\Gamma + \|p_p^{k-1}\|_\Gamma + \|\mathbf{u}_p^{k-1} \cdot \mathbf{n}_p\|_\Gamma) .$$

Square both sides and integrate over the interval $(0, t)$ for a.e. $t \in (0, T]$ to obtain

$$\frac{\beta^2}{C_d} \int_0^t \|p_f^k\|_{\Omega_f}^2 \, ds \le \int_0^t (\|\mathbf{u}_f^k\|_{\Omega_f}^2 + \|D(\mathbf{u}_f^k)\|_{\Omega_f}^2 + \sum_{j=1}^{d-1} \|\mathbf{u}_f^k \cdot \mathbf{t}_j\|_\Gamma^2 + \|p_p^{k-1}\|_\Gamma^2 + \|\mathbf{u}_p^{k-1} \cdot \mathbf{n}_p\|_\Gamma^2) \, ds , \quad (3.32)$$

where $C_d = (d + 3)(1 + C_*^{-1}\widehat{C})^2 > 0$. As $p_p^{k-1} \in H^1(\Omega_p)$ (see Remark 3.1), using the trace theorem we have $\|p_p^{k-1}\|_\Gamma \le \|p_p^{k-1}\|_{1,\Omega_p}^{1/2} \|p_p^{k-1}\|_{\Omega_p}^{1/2}$. Thus (3.32) becomes

$$\frac{\beta^2}{C_d} \int_0^t \|p_f^k\|_{\Omega_f}^2 \, ds \le \int_0^t (\|\mathbf{u}_f^k\|_{\Omega_f}^2 + \|D(\mathbf{u}_f^k)\|_{\Omega_f}^2 + \sum_{j=1}^{d-1} \|\mathbf{u}_f^k \cdot \mathbf{t}_j\|_\Gamma^2 + \|p_p^{k-1}\|_{1,\Omega_p} \|p_p^{k-1}\|_{\Omega_p} + \|\mathbf{u}_p^{k-1} \cdot \mathbf{n}_p\|_\Gamma^2) \, ds , \quad (3.33)$$

where $\|p_p^{k-1}\|_{1,\Omega_p} < \infty$, since $p_p^{k-1} \in H^1(\Omega_p)$. Because $\mathbf{u}_f^k$, $D(\mathbf{u}_f^k)$, $\mathbf{u}_f^k \cdot \mathbf{t}_j$, p_p^k and $\mathbf{u}_p^k \cdot \mathbf{n}_p$ tend to 0 in $L^\infty(0, T; \mathbf{L}^2(\Omega_f))$, $L^2(0, T; \mathbf{L}^2(\Omega_f))$, $L^2(0, T; L^2(\Gamma))$, $L^\infty(0, T; L^2(\Omega_p))$ and $L^2(0, T; L^2(\Gamma))$, respectively, as $k \to \infty$, (3.33) implies $\int_0^t \|p_f^k\|^2 ds$ converges to 0 as $k \to \infty$. Hence p_f^k tends to 0 in $L^2(0, T; L^2(\Omega_f))$ as $k \to \infty$. □

Remark 3.2. *When $\alpha_p = \alpha_f$, the proof can be carried out in a similar manner except that the use of Gronwall lemma is no longer necessary.*

Remark 3.3. *The choice of the Robin parameters, α_f and α_p, depends on the physical parameters of the problem and its discretization (i.e., the mesh size and time step size). For the case where a unique physics is considered on the whole domain, Robin parameters can be optimized by minimizing the convergence factor of the SWR algorithm in the Fourier transformed domain*

as proposed in [30]. Such an approach is called optimized Schwarz waveform relaxation (OSWR). For the stationary Stokes-Darcy system, optimization of the Robin parameters was studied in the framework of optimized Schwarz methods in [18, 31], again by means of Fourier analysis. However, for the time-dependent Stokes-Darcy coupling, it is not clear how to choose the Robin parameters in an optimal way; direct application of OSWR to the multiphysics system may not give desired numerical results in terms of accuracy of numerical solutions. We shall discuss various choices of the Robin parameters and their numerical performance in Section 5.

Remark 3.4. *A straightforward extension of the optimized Schwarz methods in [18, 31] for the stationary Stokes-Darcy system to the time-dependent case is to first discretize the equations in time implicitly, then perform the iterative algorithm at each time step. In this work, a different approach is considered by deriving the space-time interface problem associated with the Robin transmission conditions; solving such an interface problem iteratively involves the solution of time-dependent subdomain problems over the whole time interval at each iteration. Consequently, nonmatching time discretizations can be used in the subdomains which will be discussed in the next section.*

4. The semi-discrete, nonconforming in time,SWR algorithm

As the interface problem (3.11) is global-in-time, we can use different time step sizes in the Stokes and Darcy regions. The advantage of using nonconforming time grids is that time discretization can be selectively refined for a subproblem where the error in the solution is likely to be larger. In the following, we shall introduce L^2 projection functions to exchange data on the space-time interface between different time grids and prove the convergence of the time discretized SWR algorithm with nonconforming time grids.

Let τ_f be a partition of time interval $(0, T)$ into subintervals for the Stokes domain. We denote the time interval $(t_f^{m-1}, t_f^m]$ by J_f^m and the step size by $\Delta t_f^m := t_f^m - t_f^{m-1}$ for $m = 1, ..., M_f$. Denote the space of piecewise constant

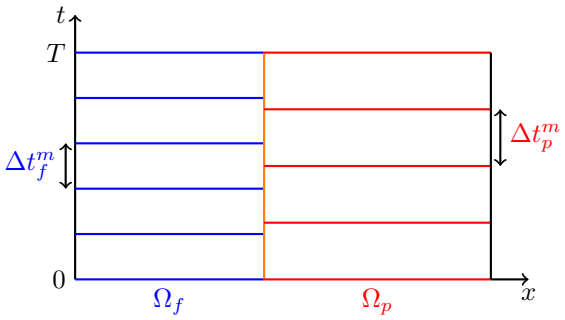

Figure 2: Nonconforming time grids.

functions in time on grid τ_f with values in W by $P_0(\tau_f, W)$, where $W = L^2(\Gamma)$:

$$P_0(\tau_f, W) = \{\phi : (0,T) \to W, \phi \text{ is constant on } J_f^m \quad \forall m = 1, ..., M_f\}.$$

We define τ_p, M_p, J_p^n and Δt_p^n similarly for the Darcy domain. In order to exchange data on the space-time interface between different time grids, we define the L^2 projection $\Pi_{p,f}$ from $P_0(\tau_f, W)$ onto $P_0(\tau_p, W)$ [30, 38]:

$$\Pi_{p,f}(\phi)|_{J_p^n} = \frac{1}{|J_p^n|} \sum_{l=1}^{M_f} \int_{J_p^n \cap J_f^l} \phi. \tag{4.1}$$

The projection $\Pi_{f,p}$ from $P_0(\tau_p, W)$ onto $P_0(\tau_f, W)$ is also defined similarly. We use the algorithm described in [30] for effectively performing these projections.

Remark 4.1. *Different subdomain time steps for the Stokes-Darcy system have also been studied in [53, 52] in which the time step size in the Stokes region is an integral multiple of the time step size in the Darcy region. These methods are non-iterative by using an explicit method for the coupling terms, and the key issue is how to achieve desired accuracy and stability properties. Here we propose the iterative SWR algorithm which enables the use of arbitrarily different time step sizes in the subdomains; the interface conditions on nonconforming time grids are enforced using the mentioned L^2 projection. The method is fully implicit in time, thus considerably large time step sizes are possible without affecting stability.*

Using the backward Euler method, the semi-discrete Stokes-Darcy system with Robin transmission conditions on Γ is given by: for $m = 1, ..., M_f$

$$\mathbf{u}_f^m - \mathbf{u}_f^{m-1} + \Delta t_f^m(-2\nu_f \nabla \cdot D(\mathbf{u}_f^m) + \nabla p_f^m I) \;=\; \int_{J_f^m} \mathbf{f}_f \, dt \quad \text{in } \Omega_f \tag{4.2}$$

$$\nabla \cdot \mathbf{u}_f^m \;=\; 0 \quad \text{in } \Omega_f \,, \tag{4.3}$$

$$\Delta t_f^m \left(\mathbf{n}_f \cdot (p_f^m \mathbf{I} - 2\nu_f D(\mathbf{u}_f^m)) \cdot \mathbf{n}_f - \alpha_f \mathbf{u}_f^m \cdot \mathbf{n}_f \right) = \int_{J_f^m} \Pi_{f,p} \left(p_p + \alpha_f \mathbf{u}_p \cdot \mathbf{n}_p \right) \, dt \text{ on } \Gamma, \tag{4.4}$$

and for $n = 1, ..., M_p$

$$\nu_p \mathbf{u}_p^n + \nabla p_p^n \;=\; 0 \quad \text{in } \Omega_p \,, \tag{4.5}$$

$$s_0(p_p^n - p_p^{n-1}) + \Delta t_p^n \nabla \cdot \mathbf{u}_p^n \;=\; \int_{J_p^n} f_p dt \quad \text{in } \Omega_p \,, \tag{4.6}$$

$$\Delta t_p^n \left(p_p^n - \alpha_p \mathbf{u}_p^n \cdot \mathbf{n}_p \right) = \int_{J_p^n} \Pi_{p,f} \left(\mathbf{n}_f \cdot (p_f \mathbf{I} - 2\nu_f D(\mathbf{u}_f)) \mathbf{n}_f + \alpha_p \mathbf{u}_f \cdot \mathbf{n}_f \right) dt \quad \text{on } \Gamma \,, \tag{4.7}$$

where $(\mathbf{u}_f, p_f) = (\mathbf{u}_f^m, p_f^m)_{m=1}^{M_f}$ satisfies the boundary conditions (2.3), (2.11) and the initial condition $\mathbf{u}_f^0 = \mathbf{u}_{f0}$; and $(\mathbf{u}_p, p_p) = (\mathbf{u}_p^n, p_p^n)_{n=1}^{M_p}$ satisfies the boundary condition (2.7) and the initial condition $p_p^0 = p_{p0}$. The semi-discrete SWR algorithm is then written as follows: in the kth iteration step, we solve

$$\mathbf{u}_f^{k,m} - \mathbf{u}_f^{k,m-1} - \Delta t_f^m \nabla \cdot (2\nu_f D(\mathbf{u}_f^{k.m}) - p_f^{k,m} I) \;=\; \int_{J_f^m} \mathbf{f}_f \, dt \text{ in } \Omega_f \tag{4.8}$$

$$\nabla \cdot \mathbf{u}_f^{k,m} \;=\; 0 \quad \text{in } \Omega_f \,, \tag{4.9}$$

$$\Delta t_f^m \left(\mathbf{n}_f^k \cdot (p_f^{k,m} \mathbf{I} - 2\nu_f D(\mathbf{u}_f^{k,m})) \cdot \mathbf{n}_f - \alpha_f \mathbf{u}_f^{k,m} \cdot \mathbf{n}_f \right) = \int_{J_f^m} \Pi_{f,p} \left(p_p^{k-1} + \alpha_f \mathbf{u}_p^{k-1} \cdot \mathbf{n}_p \right) \, dt \quad \text{on } \Gamma \tag{4.10}$$

for $(\mathbf{u}_f^k, p_f^k) = (\mathbf{u}_f^{k,m}, p_f^{k,m})_{m=1}^{M_f}$ satisfying (2.3), (2.11), where $\mathbf{u}_f^{k,0} = \mathbf{u}_{f0}$,

$\mathbf{u}_f^{k,m} := \mathbf{u}_f^k|_{J_f^m}, p_f^{k,m} := p_f^k|_{J_f^m}$ for $m = 1, ..., M_f$, and

$$\nu_p \mathbf{u}_p^{k,n} + \nabla p_p^{k,n} = 0 \quad \text{in } \Omega_p\,, \tag{4.11}$$

$$s_0(p_p^{k,n} - p_p^{k,n-1}) + \Delta t_p^n \nabla \cdot \mathbf{u}_p^{k,n} = \int_{J_p^n} \mathbf{f}_p dt \quad \text{in } \Omega_p\,, \tag{4.12}$$

$$\begin{aligned} &\Delta t_p^n \left(p_p^{k,n} - \alpha_p \mathbf{u}_p^{k,n} \cdot \mathbf{n}_p \right) \\ &= \int_{J_p^n} \Pi_{p,f} \left(\mathbf{n}_f \cdot (p_f^{k-1}\mathbf{I} - 2\nu_f D(\mathbf{u}_f^{k-1}))\mathbf{n}_f + \alpha_p \mathbf{u}_f^{k-1} \cdot \mathbf{n}_f \right) dt \\ &\qquad\qquad \text{on } \Gamma \end{aligned} \tag{4.13}$$

for $(\mathbf{u}_p^k, p_p^k) = (\mathbf{u}_p^{k,n}, p_p^{k,n})_{n=1}^{M_p}$ satisfying (2.7), where $p_p^{k,0} = p_{p0}$, $\mathbf{u}_p^{k,n} := \mathbf{u}_p^k|_{J_p^n}, p_p^{k,n} := p_p^k|_{J_p^n}$ for $n = 1, ..., M_p$. We show in the following theorem that as $k \to \infty$, the weak solution to (4.2)-(4.7) converges to the weak solution of (4.8)-(4.13).

Theorem 4.1. *Assume that $\alpha_f = \alpha_p > 0$. If initial guess values $(\mathbf{u}_f^0, p_f^0, \mathbf{u}_p^0, p_p^0)$ are chosen such that the Robin-Robin conditions (4.10), (4.13) are well-defined in $L^2(\Gamma)$, the weak formulation* (4.8)-(4.13) *defines a unique sequence of iterates*

$$(\mathbf{u}_f^k, p_f^k, \mathbf{u}_p^k, p_p^k) \in P_0(\tau_f; \boldsymbol{X}_f) \times P_0(\tau_f; Q_f) \times P_0(\tau_p; \boldsymbol{X}_p) \times P_0(\tau_p; Q_p)$$

that converges to the weak solution of (4.2)-(4.7).

Proof. As the equations are linear, we let $\mathbf{f}_f = \mathbf{u}_{f0} = \mathbf{0}$, $f_p = p_{p0} = 0$ and derive the energy estimates as in the proof of Theorem 3.1. First, we multiply (4.8), (4.9) by $\mathbf{u}_f^{k,m}$ and $p_f^{k,m}$, respectively, integrate them over Ω_f and use (2.11). Then add two resulting equations and use (3.22) to obtain

$$\begin{aligned} &(\mathbf{u}_f^{k,m}, \mathbf{u}_f^{k,m})_{\Omega_f} - (\mathbf{u}_f^{k,m-1}, \mathbf{u}_f^{k,m})_{\Omega_f} + 2\Delta t_f^m \nu_f \|D(\mathbf{u}_f^{k,m})\|_{\Omega_f}^2 \\ &\qquad + \sum_{j=1}^{d-1} c_{BJS} \Delta t_f^m \|\mathbf{u}_f^{k,m} \cdot \mathbf{t}_j\|_{\Omega_f}^2 \\ &\qquad + \frac{\Delta t_f^m}{2(\alpha_f + \alpha_p)} \|\mathbf{n}_f \cdot (p_f^{k,m}\mathbf{I} - 2\nu_f D(\mathbf{u}_f^{k,m})) \cdot \mathbf{n}_f + \alpha_p \mathbf{u}_f^{k,m} \cdot \mathbf{n}_f\|_\Gamma^2 \\ \le\ &\frac{\Delta t_f^m}{2(\alpha_f + \alpha_p)} \|\mathbf{n}_f \cdot (p_f^{k,m}\mathbf{I} - 2\nu_f D(\mathbf{u}_f^{k,m})) \cdot \mathbf{n}_f - \alpha_f \mathbf{u}_f^{k,m} \cdot \mathbf{n}_f\|_\Gamma^2 \\ &\qquad + \frac{\Delta t_f^m (\alpha_p - \alpha_f)}{2} \|\mathbf{u}_f^{k,m} \cdot \mathbf{n}_f\|_\Gamma^2. \end{aligned}$$

Using Cauchy-Schwarz inequality and $\frac{1}{2}(a^2-b^2) \le a^2 - ab$, we obtain

$$\begin{aligned}
&\frac{1}{2}\left(\|\mathbf{u}_f^{k,m}\|_{\Omega_f}^2 - \|\mathbf{u}_f^{k,m-1}\|_{\Omega_f}^2\right) + \int_{J_f^m} 2\nu_f \|D(\mathbf{u}_f^k)\|_{\Omega_f}^2 \, dt \\
&\qquad + \sum_{j=1}^{d-1} c_{BJS} \int_{J_f^m} \|\mathbf{u}_f^k \cdot \mathbf{t}_j\|_{\Omega_f}^2 \, dt \\
&\qquad + \frac{1}{2(\alpha_f+\alpha_p)} \int_{J_f^m} \|\mathbf{n}_f \cdot (p_f^k \mathbf{I} - 2\nu_f D(\mathbf{u}_f^k)) \cdot \mathbf{n}_f + \alpha_p \mathbf{u}_f^k \cdot \mathbf{n}_f\|_\Gamma^2 \, dt \\
&\le \frac{1}{2(\alpha_f+\alpha_p)} \int_{J_f^m} \|\mathbf{n}_f \cdot (p_f^k \mathbf{I} - 2\nu_f D(\mathbf{u}_f^k)) \cdot \mathbf{n}_f - \alpha_f \mathbf{u}_f^k \cdot \mathbf{n}_f\|_\Gamma^2 \, dt \\
&\qquad + \frac{\alpha_p - \alpha_f}{2} \int_{J_f^m} \|\mathbf{u}_f^k \cdot \mathbf{n}_f\|_\Gamma^2 \, dt. \qquad (4.14)
\end{aligned}$$

Similarly, multiply (4.11), (4.12) by $\mathbf{u}_p^{k,n}$ and $p_p^{k,n}$, respectively, integrate over Ω_p, add the two results and use (3.23) to have

$$\begin{aligned}
&\nu_p \int_{J_p^n} \|\mathbf{u}_p^k\|_{\Omega_p}^2 \, dt + \frac{s_0}{2}\left(\|p_p^{k,n}\|_{\Omega_p}^2 - \|p_p^{k,n-1}\|_{\Omega_p}^2\right) \\
&\qquad + \frac{1}{2(\alpha_f+\alpha_p)} \int_{J_p^n} \|p_p^k + \alpha_f \mathbf{u}_p^k \cdot \mathbf{n}_p\|_\Gamma^2 \, dt \\
&\le \frac{1}{2(\alpha_f+\alpha_p)} \int_{J_p^n} \|p_p^k - \alpha_p \mathbf{u}_p^k \cdot \mathbf{n}_p\|_\Gamma^2 \, dt - \frac{\alpha_p - \alpha_f}{2} \int_{J_p^n} \|\mathbf{u}_p^k \cdot \mathbf{n}_p\|_\Gamma^2 \, dt. \qquad (4.15)
\end{aligned}$$

We cannot use Gronwall's lemma as in the continuous case because of the global-in-time projections $\Pi_{f,p}$ and $\Pi_{p,f}$. Hence, we make the assumption that $\alpha_f = \alpha_p$ to cancel the last terms of (4.14) and (4.15). Summing (4.14) and (4.15) over the subintervals in $(0, t_f^m]$ and $(0, t_p^n]$, respectively, yields

$$\begin{aligned}
&\frac{1}{2}\|\mathbf{u}_f^{k,m}\|_{\Omega_f}^2 + \int_0^{t_f^m} 2\nu_f \|D(\mathbf{u}_f^k)\|_{\Omega_f}^2 \, dt + \sum_{j=1}^{d-1} c_{BJS} \int_0^{t_f^m} \|\mathbf{u}_f^k \cdot \mathbf{t}_j\|_{\Omega_f}^2 \, dt \\
&\qquad + \frac{1}{2(\alpha_f+\alpha_p)} \int_0^{t_f^m} \|\mathbf{n}_f \cdot (p_f^k \mathbf{I} - 2\nu_f D(\mathbf{u}_f^k)) \cdot \mathbf{n}_f + \alpha_p \mathbf{u}_f^k \cdot \mathbf{n}_f\|_\Gamma^2 \, dt \\
&\le \frac{1}{2(\alpha_f+\alpha_p)} \int_0^{t_f^m} \|\mathbf{n}_f \cdot (p_f^k \mathbf{I} - 2\nu_f D(\mathbf{u}_f^k)) \cdot \mathbf{n}_f - \alpha_f \mathbf{u}_f^k \cdot \mathbf{n}_f\|_\Gamma^2 \, dt, \qquad (4.16)
\end{aligned}$$

and

$$\begin{aligned}
&\nu_p \int_0^{t_p^n} \|\mathbf{u}_p^k\|_{\Omega_p}^2 \, dt + \frac{s_0}{2}\|p_p^{k,n}\|_{\Omega_p}^2 + \frac{1}{2(\alpha_f+\alpha_p)} \int_0^{t_p^n} \|p_p^k + \alpha_f \mathbf{u}_p^k \cdot \mathbf{n}_p\|_\Gamma^2 \, dt \\
&\qquad \le \frac{1}{2(\alpha_f+\alpha_p)} \int_0^{t_p^n} \|p_p^k - \alpha_p \mathbf{u}_p^k \cdot \mathbf{n}_p\|_\Gamma^2 \, dt. \qquad (4.17)
\end{aligned}$$

Adding (4.16) and (4.17), and using the Robin conditions (4.10) and (4.13), we obtain

$$\begin{aligned}
&\frac{1}{2}\|\mathbf{u}_f^{k,m}\|^2_{\Omega_f} + \int_0^{t_f^m} 2\nu_f \|D(\mathbf{u}_f^k)\|^2_{\Omega_f}\, dt \\
&\qquad + \sum_{j=1}^{d-1} c_{BJS} \int_0^{t_f^m} \|\mathbf{u}_f^k \cdot \mathbf{t}_j\|^2_{\Omega_f}\, dt + \nu_p \int_0^{t_p^n} \|\mathbf{u}_p^k\|^2_{\Omega_p}\, dt \\
&\qquad + \frac{s_0}{2}\|p_p^{k,n}\|^2_{\Omega_p} + \frac{1}{2(\alpha_f+\alpha_p)} \int_0^{t_p^n} \|p_p^k + \alpha_f \mathbf{u}_p^k \cdot \mathbf{n}_p\|^2_\Gamma\, dt \\
&\qquad + \frac{1}{2(\alpha_f+\alpha_p)} \int_0^{t_f^m} \|\mathbf{n}_f \cdot (p_f^k \mathbf{I} - 2\nu_f D(\mathbf{u}_f^k)) \cdot \mathbf{n}_f + \alpha_p \mathbf{u}_f^k \cdot \mathbf{n}_f\|^2_\Gamma\, dt \\
&\leq \frac{1}{2(\alpha_f+\alpha_p)} \int_0^{t_f^m} \|\Pi_{f,p}(p_p^{k-1} + \alpha_f \mathbf{u}_p^{k-1} \cdot \mathbf{n}_p)\|^2_\Gamma\, dt \\
&+ \frac{1}{2(\alpha_f+\alpha_p)} \int_0^{t_p^n} \|\Pi_{p,f}(\mathbf{n}_f \cdot (p_f^{k-1}\mathbf{I} - 2\nu_f D(\mathbf{u}_f^{k-1})) \cdot \mathbf{n}_f + \alpha_p \mathbf{u}_f^{k-1} \cdot \mathbf{n}_f)\|^2_\Gamma\ \ dt \\
&\leq \frac{1}{2(\alpha_f+\alpha_p)} \int_0^{t_f^m} \|p_p^{k-1} + \alpha_f \mathbf{u}_p^{k-1} \cdot \mathbf{n}_p\|^2_\Gamma\, dt \\
&+ \frac{1}{2(\alpha_f+\alpha_p)} \int_0^{t_p^n} \|\mathbf{n}_f \cdot (p_f^{k-1}\mathbf{I} - 2\nu_f D(\mathbf{u}_f^{k-1})) \cdot \mathbf{n}_f + \alpha_p \mathbf{u}_f^{k-1} \cdot \mathbf{n}_f\|^2_\Gamma\, dt\,. \qquad (4.18)
\end{aligned}$$

We set $m = M_f$ and $n = M_p$ then $t_f^{M_f} = t_p^{M_p} = T$. Now (4.18) becomes

$$\begin{aligned}
&\frac{1}{2}\|\mathbf{u}_f^{k,M_f}\|^2_{\Omega_f} + \int_0^T 2\nu_f \|D(\mathbf{u}_f^k)\|^2_{\Omega_f}\, dt + \sum_{j=1}^{d-1} c_{BJS} \int_0^T \|\mathbf{u}_f^k \cdot \mathbf{t}_j\|^2_{\Omega_f}\, dt \\
&+ \nu_p \int_0^T \|\mathbf{u}_p^k\|^2_{\Omega_p}\, dt + \frac{s_0}{2}\|p_p^{k,M_p}\|^2_{\Omega_p} + \frac{1}{2(\alpha_f+\alpha_p)} \int_0^T \|p_p^k + \alpha_f \mathbf{u}_p^k \cdot \mathbf{n}_p\|^2_\Gamma\, dt \\
&+ \frac{1}{2(\alpha_f+\alpha_p)} \int_0^T \|\mathbf{n}_f \cdot (p_f^k \mathbf{I} - 2\nu_f D(\mathbf{u}_f^k)) \cdot \mathbf{n}_f + \alpha_p \mathbf{u}_f^k \cdot \mathbf{n}_f\|^2_\Gamma\, dt \\
&\leq \frac{1}{2(\alpha_f+\alpha_p)} \int_0^T \|p_p^{k-1} + \alpha_f \mathbf{u}_p^{k-1} \cdot \mathbf{n}_p\|^2_\Gamma\, dt \\
&+ \frac{1}{2(\alpha_f+\alpha_p)} \int_0^T \|\mathbf{n}_f \cdot (p_f^{k-1}\mathbf{I} - 2\nu_f D(\mathbf{u}_f^{k-1})) \cdot \mathbf{n}_f + \alpha_p \mathbf{u}_f^{k-1} \cdot \mathbf{n}_f\|^2_\Gamma\, dt\,.
\end{aligned}$$

Then, for all $k > 0$

$$\begin{aligned}
&\frac{1}{2}\|\mathbf{u}_f^{k,M_f}\|^2_{\Omega_f} + \int_0^T 2\nu_f \|D(\mathbf{u}_f^k)\|^2_{\Omega_f}\, dt + \sum_{j=1}^{d-1} c_{BJS} \int_0^T \|\mathbf{u}_f^k \cdot \mathbf{t}_j\|^2_{\Omega_f}\, dt \\
&\qquad + \nu_p \int_0^T \|\mathbf{u}_p^k\|^2_{\Omega_p}\, dt + \frac{s_0}{2}\|p_p^{k,M_p}\|^2_{\Omega_p} + B^k \;\leq\; B^{k-1},
\end{aligned}$$

where

$$B^k = \frac{1}{2(\alpha_f+\alpha_p)} \int_0^T \|\mathbf{n}_f\cdot(p_f^k\mathbf{I}-2\nu_f D(\mathbf{u}_f^k))\cdot\mathbf{n}_f+\alpha_p\mathbf{u}_f^k\cdot\mathbf{n}_f\|_\Gamma^2+\|p_p^k+\alpha_f\mathbf{u}_p^k\cdot\mathbf{n}_p\|_\Gamma^2 \, dt\,.$$

We sum over the iterates k to obtain that $\|\mathbf{u}_f^{k,M_f}\|_{\Omega_f}^2$, $\int_0^T \|D(\mathbf{u}_f^k)\|_{\Omega_f}^2 dt$, $\sum_{j=1}^{d-1}\int_0^T \|\mathbf{u}_f^k\cdot\mathbf{t}_j\|_{\Omega_f}^2 dt$, $\int_0^T \|\mathbf{u}_p^k\|_{\Omega_p}^2 dt$ and $\|p_p^{k,M_p}\|_{\Omega_p}^2$ converge to 0 as $k\to\infty$. This implies $\int_0^{t_f^m} \|D(\mathbf{u}_f^k)\|_{\Omega_f}^2 dt$, $\sum_{j=1}^{d-1}\int_0^{t_f^m} \|\mathbf{u}_f^k\cdot\mathbf{t}_j\|_{\Omega_f}^2 dt$ converge to 0 as $k\to\infty$ for $m=1,....,M_f$ and $\int_0^{t_p^n} \|\mathbf{u}_p^k\|_{\Omega_p}^2 dt$ converges to 0 as $k\to\infty$ for $n=1,....,M_p$. From Poincaré-Friedrichs inequality and Korn's inequality, we have $\|\mathbf{u}_f^{k,m}\|_{\Omega_f}^2 \le \overline{C}_{PF}\|D(\mathbf{u}_f^{k,m})\|_{\Omega_f}^2$ for some constant $\overline{C}_{PF}>0$. This implies $\int_0^{t_f^m} \|\mathbf{u}_f^k\|_{\Omega_f}^2 dt$ converges to 0 as $k\to\infty$ for $m=1,....,M_f$.

To show the convergence of $p_p^{k,n}$, we multiply (4.11) by $\nabla p_p^{k,m}$, integrate over Ω_p and use Cauchy-Schwarz inequality to obtain

$$\|\nabla p_p^{k,n}\|_{\Omega_p}^2 = -\nu_p(\mathbf{u}_p^{k,n},\nabla p_p^{k,n}) \le \nu_p\|\mathbf{u}_p^{k,n}\|_{\Omega_p}\|\nabla p_p^{k,n}\|_{\Omega_p}\,.$$

Since $p_p^{k,n}\in H^1(\Omega_p)$ (see remark 3.1), using Poincaré-Friedrichs inequality,

$$C_{PF}^{-1}\|p_p^{k,n}\|_{\Omega_p} \le \|\nabla p_p^{k,n}\|_{\Omega_p} \le \nu_p\|\mathbf{u}_p^{k,n}\|_{\Omega_p}, \tag{4.19}$$

for some constant $C_{PF}>0$. Squaring all sides and integrating them over $(0,t_p^n]$, we have that $\int_0^{t_p^n}\|p_p^k\|_{\Omega_p}^2 dt$ converges to 0 as $k\to\infty$ for $n=1,....,M_p$. Similarly, we multiply (4.12) by $\nabla\cdot\mathbf{u}_p^{k,n}$ and integrate over Ω_p to obtain

$$\begin{aligned}\Delta t_p^n\|\nabla\cdot\mathbf{u}_p^{k,n}\|_{\Omega_p}^2 &= -(s_0(p_p^{k,n}-p_p^{k,n-1}),\nabla\cdot\mathbf{u}_p^{k,n})_{\Omega_p}\\ &\le s_0\|p_p^{k,n}-p_p^{k,n-1}\|_{\Omega_p}\|\nabla\cdot\mathbf{u}_p^{k,n}\|_{\Omega_p}\,,\end{aligned}$$

which yields

$$\Delta t_p^n\|\nabla\cdot\mathbf{u}_p^{k,n}\|_{\Omega_p} \le s_0\|p_p^{k,n}-p_p^{k,n-1}\|_{\Omega_p} \le s_0\left(\|p_p^{k,n}\|_{\Omega_p}+\|p_p^{k,n-1}\|_{\Omega_p}\right).$$

Now, squaring all sides, integrating them over $(0,t_p^n]$ and the convergence of $\int_0^{t_p^n}\|p_p^k\|_{\Omega_p}^2 dt$ yield that $\int_0^{t_p^n}\|\nabla\cdot\mathbf{u}_p^k\|_{\Omega_p}^2 dt$ converges to 0 as $k\to\infty$ for $n=1,....,M_p$. Also, this result together with the convergence of $\int_0^{t_p^n}\|\mathbf{u}_p^k\|_{\Omega_p}^2 dt$ implies that $\int_0^{t_p^n}\|\mathbf{u}_p^k\|_{\mathbf{H}^{\mathrm{div}}(\Omega_p)}^2 dt$ converges to 0 as $k\to\infty$ for $n=1,.....,M_p$.

For the convergence of $p_f^{k,m}$ we multiply (4.8) by $\mathbf{v}_f \in \mathbf{V}_f$, integrate over Ω_f and proceed similarly to the continuous case to have

$$\frac{1}{\Delta t_f^m}\|\mathbf{u}_f^{k,m} - \mathbf{u}_f^{k,m-1}\|_{\mathbf{X}_f^{h*}} \leq C_*^{-1}C(\,\|\mathbf{u}_f^{k,m}\|_{\Omega_f} + \|D(\mathbf{u}_f^{k,m})\|_{\Omega_f} + \sum_{j=1}^{d-1}\|\mathbf{u}_f^{k,m}\cdot\mathbf{t}_j\|_\Gamma + \|\Pi_{f,p}(p_p^{k-1,m} + \alpha_p\mathbf{u}_p^{k-1,m}\cdot\mathbf{n}_p)\|_\Gamma\,). \quad (4.20)$$

Next, we multiply (4.8) by $\mathbf{v}_f \in \mathbf{X}_f$ and integrate over Ω_f. And then isolate the pressure term, divide by $\|\nabla\mathbf{v}_f\|$, take supremum over $\mathbf{v}_f \in \mathbf{X}_f$. Then, using the inf-sup condition (2.12) and estimate (4.20),

$$\beta\|p_f^{k,m}\|_{\Omega_f} \leq (1 + C_*^{-1}C)(\,\|\mathbf{u}_f^{k,m}\|_{\Omega_f} + \|D(\mathbf{u}_f^{k,m})\|_{\Omega_f} + \sum_{j=1}^{d-1}\|\mathbf{u}_f^{k,m}\cdot\mathbf{t}_j\|_\Gamma + \|p_p^{k-1,m}\|_\Gamma + \alpha_p\|\mathbf{u}_p^{k-1,m}\cdot\mathbf{n}_p\|_\Gamma\,),$$

for some $\beta > 0$. Square both sides and integrate over $(0, t_f^m]$. Then, for some $t_p^n \geq t_f^m$, we have

$$\beta^2\int_0^{t_f^m}\|p_f^k\|_{\Omega_f}^2\,dt \leq (d+3)(1+C_*^{-1}C)^2\left(\int_0^{t_f^m}\|\mathbf{u}_f^k\|_{\Omega_f}^2 + \|D(\mathbf{u}_f^k)\|_{\Omega_f}^2 + \sum_{j=1}^{d-1}\|\mathbf{u}_f^k\cdot\mathbf{t}_j\|_\Gamma^2\,dt + \int_0^{t_p^n}\|p_p^{k-1}\|_\Gamma^2 + \alpha_p\|\mathbf{u}_p^{k-1}\cdot\mathbf{n}_p\|_\Gamma^2\,dt\right). \quad (4.21)$$

As $p_p^{k-1} \in H^1(\Omega_p)$, using the trace theorem, we have $\|p_p^{k-1}\|_\Gamma \leq \|p_p^{k-1}\|_{1,\Omega_p}^{1/2}\|p_p^{k-1}\|_{\Omega_p}^{1/2}$. Also, using $\|\mathbf{u}_p^{k-1}\cdot\mathbf{n}_p\|_\Gamma \leq C\|\mathbf{u}_p^{k-1}\|_{\mathbf{H}^{\mathrm{div}}(\Omega_p)}$, (4.21) becomes

$$\beta^2\int_0^{t_f^m}\|p_f^k\|^2\,dt \leq C\left(\int_0^{t_f^m}\|\mathbf{u}_f^k\|_{\Omega_f}^2 + \|D(\mathbf{u}_f^k)\|_{\Omega_f}^2 + \sum_{j=1}^{d-1}\|\mathbf{u}_f^k\cdot\mathbf{t}_j\|_\Gamma^2\,dt + \int_0^{t_p^n}\|p_p^{k-1}\|_{1,\Omega_p}\|p_p^{k-1}\|_{\Omega_p} + \|\mathbf{u}_p^{k-1}\|_{\mathbf{H}^{\mathrm{div}}(\Omega_p)}^2\,dt\right). \quad (4.22)$$

As $p_p^{k-1} \in H^1(\Omega_p)$, $\|p_p^{k-1}\|_{1,\Omega_p} < \infty$. Therefore, the convergence of $\int_0^{t_f^m}\|p_f^k\|^2 dt$ to 0 is obtained, since each term in the right hand side of (4.22) converges to 0 as $k \to \infty$ for $m = 1, ..., M_f$.

□

Remark 4.2. *The assumption that $\alpha_f = \alpha_p$ is only necessary for the convergence analysis of the semi-discrete Stokes-Darcy system with nonconforming time grids due to a technical difficulty. However, for the numerical experiments as shown in the next section, this assumption is not required and one can choose different values for the Robin parameters, $0 < \alpha_f \leq \alpha_p$, as in Theorem 3.1.*

5. Numerical results

In this section, we consider two numerical tests to investigate the convergence and efficiency of the proposed global-in-time DD algorithm. The first numerical example is a manufactured problem where the exact solution is known. The second is a physical example where a flow is driven by a pressure drop. As mentioned in Subsection 3.1, GMRES is used in the numerical experiments to solve the space-time interface problem (3.11) iteratively. We shall verify the accuracy and convergence of the numerical solutions with decreasing grid sizes and time step sizes.

5.1. Test 1

We consider a test case with a known exact solution. The subdomains chosen are $\Omega_p = (0,1) \times (0,1)$ for the porous medium and $\Omega_f = (0,1) \times (1,2)$ for the fluid domain, with the interface $\Gamma = \{(x,y) : 0 < x < 1, y = 1\}$. The exact solution is given by

$$\begin{aligned}
\mathbf{u}_f &= [(y-1)^2 x^3 (1+t^2)\ ,\ -\cos(y)e(1+t^2)], \\
p_f &= (\cos(x)e^y + y^2 - 2y + 1)(1+t^2), \\
\mathbf{u}_p &= [-x(\sin(y)e + 2(y-1))(1+t^2)\ ,\ (-\cos(y)e + (y-1)^2)(1+t^2)], \\
p_p &= (-\sin(y)e + \cos(x)e^y + y^2 - 2y + 1)(1+t^2),
\end{aligned}$$

for which the Beavers-Joseph-Saffman condition is satisfied with $\alpha = 1$. The model parameters are chosen as $\nu_f = 1, \nu_p = 1, s_0 = 1$. The initial and boundary conditions are imposed using the exact solution. Two different finite element spaces were used for numerical simulations. First, we used Taylor-Hood elements

for both $(\mathbf{u}_f, p_f)$ and $(\mathbf{u}_p, p_p$. As $\mathbf{u}_p \in H^{\text{div}}(\Omega_p)$, Taylor-Hood elements are not conforming for $(\mathbf{u}_p, p_p)$. Hence, the stabilization term $\gamma(\nabla\cdot\mathbf{u}_p, \nabla\cdot\mathbf{v}_p)$ was added to the Darcy equation (3.20) with $\gamma = 10$. Secondly, we used MINI elements for the Stokes and Raviart-Thomas of order one and P1 elements (RT1-P1) for the Darcy problem. The Robin parameters are chosen as $\alpha_f = 0.1$ and $\alpha_p = 50$. Test results using different values of Robin parameters will be discussed later. The tolerance for GMRES is set to be $\epsilon = 10^{-6}$.

First, we investigate the convergence of numerical solutions through spatial mesh refinement with nonconforming time grids. Table 1 and Table 2 show errors at $T = 0.01$ with $\Delta t_f = 0.002$ and $\Delta t_p = 0.001$ by Taylor-Hood elements for both the Stokes and Darcy problems and by MINI elements for the Stokes and RT1-P1 elements for Darcy problem, respectively. Note that for this non-physical example, the errors in the porous medium are larger, so we have chosen a small time step there while using a larger time step in the fluid domain. We observe from Tables 1 and 2 that the orders of accuracy in space are preserved with nonconforming time grids.

h		1/4	1/8	1/16	1/32
$\mathbf{u}_f$	L^2 error	8.34e-04	9.39e-05 [3.15]	1.15e-05 [3.03]	1.62e-06 [2.83]
	H^1 error	2.68e-02	5.81e-03 [2.21]	1.32e-03 [2.13]	3.38e-04 [1.97]
p_f	L^2 error	2.80e-02	5.53e-03 [2.34]	1.29e-03 [2.09]	3.91e-04 [1.73]
$\mathbf{u}_p$	L^2 error	1.11e-03	2.53e-04 [2.14]	3.84e-05 [2.72]	4.19e-06 [3.20]
	H^{div} error	2.11e-03	4.43e-04 [2.25]	9.55e-05 [2.21]	1.91e-05 [2.32]
p_p	L^2 error	2.31e-02	5.03e-03 [2.20]	1.26e-03 [1.99]	3.13e-04 [2.01]

Table 1: Errors at $T = 0.01$ by Taylor-Hood elements for the Stokes and Darcy problems using $(\Delta t_f, \Delta t_p) = (0.002, 0.001)$ and $(\alpha_f, \alpha_p) = (0.1, 50)$.

We also performed convergence tests with respect to different time steps while keeping the mesh size fixed, $h = 1/32$. We denote the coarse time step size by Δt_{coarse}. For Taylor-Hood elements, we use $\Delta t_{\text{coarse}} \in \{0.2, 0.1, 0.05, 0.0025\}$.

h		1/4	1/8	1/16	1/32
$\mathbf{u}_f$	L^2 error	9.60e-03	2.43e-03 [1.98]	5.49e-04 [2.15]	1.44e-04 [1.93]
	H^1 error	2.71e-01	1.29e-01 [1.07]	6.10e-02 [1.08]	3.15e-02 [0.95]
p_f	L^2 error	4.54e-01	1.06e-01 [2.10]	2.22e-02 [2.26]	5.63e-03 [1.98]
$\mathbf{u}_p$	L^2 error	1.99e-02	4.16e-03 [2.26]	1.01e-03 [2.04]	2.47e-04 [2.03]
	H^{div} error	2.26e-02	4.37e-03 [2.37]	1.06e-03 [2.03]	2.56e-04 [2.05]
p_p	L^2 error	2.26e-02	4.91e-03 [2.20]	1.23e-03 [1.99]	3.06e-04 [2.01]

Table 2: Errors at $T = 0.01$ by MINI elements for the Stokes and RT1-P1 elements for Darcy problem using $(\Delta t_f, \Delta t_p) = (0.002, 0.001)$ and $(\alpha_f, \alpha_p) = (0.1, 50)$.

In the case of MINI elements for the Stokes and RT1-P1 elements for the Darcy, we use $\Delta t_{\mathrm{coarse}} \in \{0.8, 0.4, 0.2, 0.1\}$. The fine time step size is given by $\Delta t_{\mathrm{fine}} = \Delta t_{\mathrm{coarse}}/2$. Consider three types of time grids as follows:

1. Coarse conforming time grids: $\Delta t_f = \Delta t_p = \Delta t_{\mathrm{coarse}}$,
2. Fine conforming time grids: $\Delta t_f = \Delta t_p = \Delta t_{\mathrm{fine}}$,
3. Nonconforming time grids: $\Delta t_f = \Delta t_{\mathrm{coarse}}$ and $\Delta t_p = \Delta t_{\mathrm{fine}}$.

In Figure 3 we show the errors at $T = 0.2$ by Taylor-Hood elements using $\alpha_f = 0.1$ and $\alpha_p = 50$. Similarly Figure 4 presents errors by MINI elements and RT1-P1 elements at $T = 0.8$ using $\alpha_f = 0.1$ and $\alpha_p = 50$ on the fixed mesh $h = 1/64$. We observe that the first order convergence is preserved with the conforming and nonconforming time grids. The errors with nonconforming time grids in the porous medium are close to those with fine conforming time grids, which is expected, as a smaller time step is used in the porous medium. We also note that the H^{div} errors of Darcy velocity are very sensitive to the Robin parameters. In Figure 5 we compare H^{div} errors of Darcy velocity at $T = 0.2$ by Taylor-Hood elements using $\alpha_p = 50$ for different values of α_f. Similarly, in Figure 6, we compare H^{div} errors of Darcy velocity at $T = 0.2$ by Taylor-Hood elements using $\alpha_f = 0.1$ for different values of α_p. After performing experiments using various pairs of (α_f, α_p), we noticed that the first order convergence with

respect to time is achieved if $\alpha_p \approx 500\alpha_f$ and $\alpha_f \leq 1$, which is the motivation for the choice of parameters $(\alpha_f, \alpha_p) = (0.1, 50)$ in most of our numerical tests. For very smaller values of α_f, we notice that the H^{div} errors of Darcy velocity for nonconforming case shift from conforming coarse to conforming fine on increasing α_p (see Figure 7). In Table 3 we compare the computer running time (in seconds) of conforming and nonconforming time grids for Taylor-Hood elements on the fixed mesh $h = 1/32$. Similarly, in Table 4, we compare the computer running time (in seconds) for MINI elements and RT1-P1 elements on the fixed mesh $h = 1/64$. We observe that using nonconforming time grids could significantly reduce the computational time while still maintaining the desired accuracy.

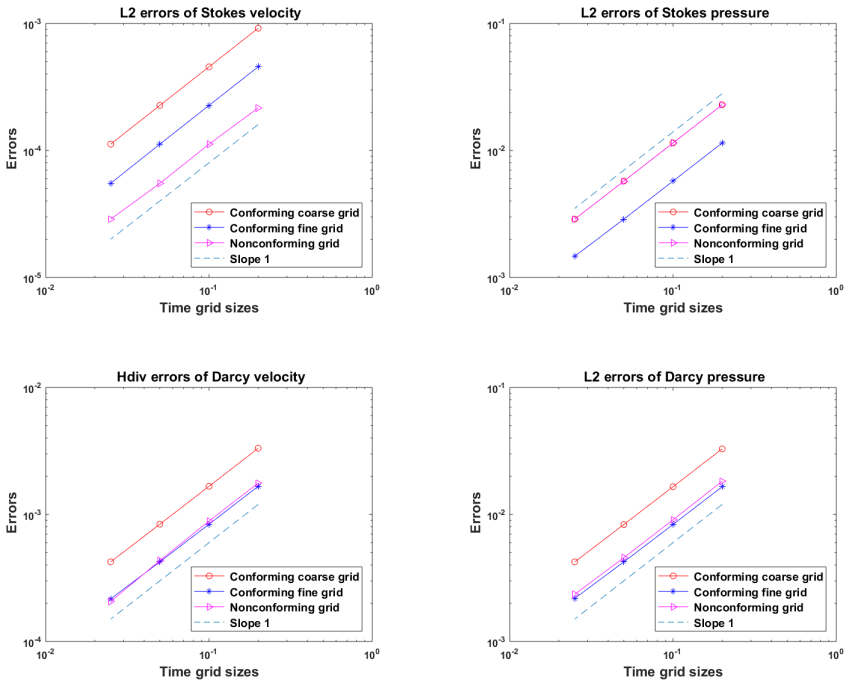

Figure 3: Errors for the Stokes and Darcy problems at T = 0.2 by Taylor-Hood elements using $(\alpha_f, \alpha_p) = (0.1, 50)$.

Δt	Conforming	Nonconforming
0.2	72	
0.1	144	77
0.05	285	153
0.025	576	314
0.0125	1114	622

Table 3: Comparison of the computer running times (in seconds) of conforming and nonconforming time grids with Taylor-Hood elements on fixed mesh $h = 1/32$ using $(\alpha_f, \alpha_p) = (0.1, 50)$.

Δt	Conforming	Nonconforming
0.8	1445	
0.4	2833	1446
0.2	5939	2871
0.1	10923	6457
0.05	22198	11244

Table 4: Comparison of the computer running times (in seconds) of conforming and nonconforming time grids with MINI elements for the Stokes and RT1-P1 element for the Darcy problems on fixed mesh $h = 1/64$ using $(\alpha_f, \alpha_p) = (0.1, 50)$.

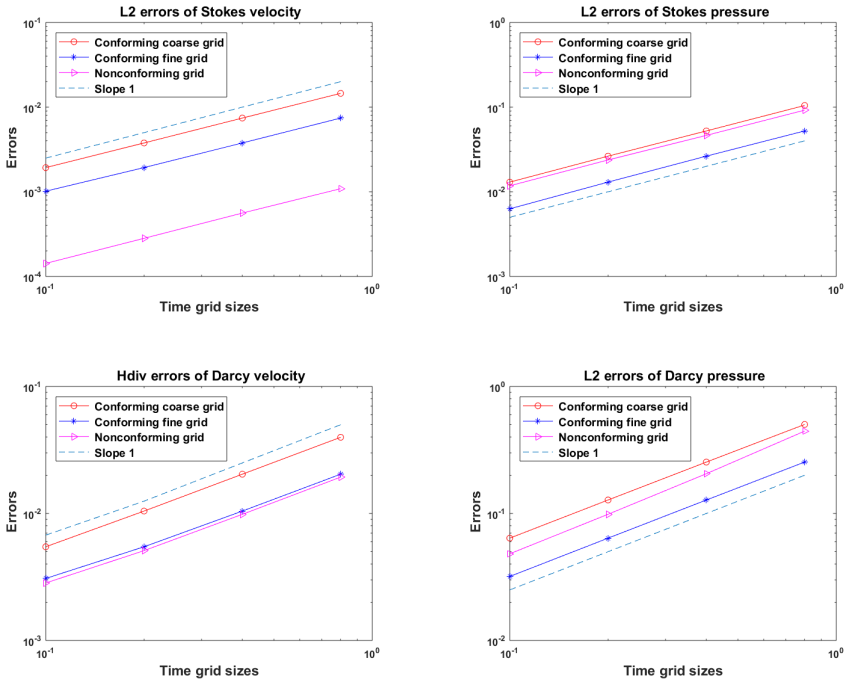

Figure 4: Errors by MINI elements for the Stokes and RT1-P1 elements for the Darcy problems at $T = 0.8$ using $(\alpha_f, \alpha_p) = (0.1, 50)$.

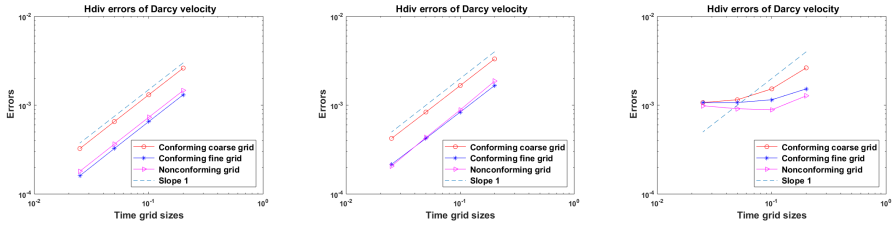

(a) $\alpha_f = 0.001$ (b) $\alpha_f = 0.1$ (c) $\alpha_f = 1$

Figure 5: H^{div} errors of Darcy velocity at T = 0.2 by Taylor-Hood elements using $\alpha_p = 50$ for different values of α_f.

5.2. Test 2

In this example, we consider a flow driven by a pressure drop in the same domain as in Test1. Let $p_{\mathrm{in}} = 1$ on the top boundary of Ω_f and $p_{\mathrm{out}} = 0$ on the bottom boundary of Ω_p. We impose the no-slip boundary condition on the left

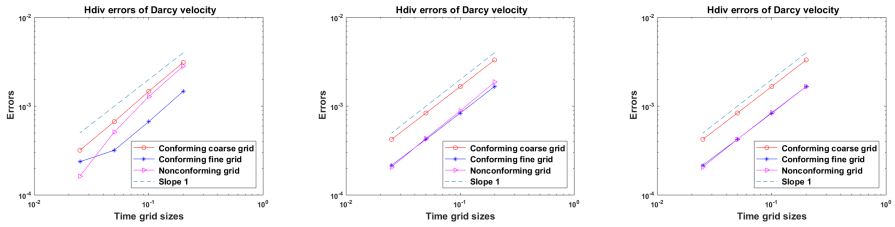

(a) $\alpha_p = 10$ (b) $\alpha_p = 50$ (c) $\alpha_p = 100$

Figure 6: H^{div} errors of Darcy velocity at T = 0.2 by Taylor-Hood elements using $\alpha_f = 0.1$ for different values of α_p.

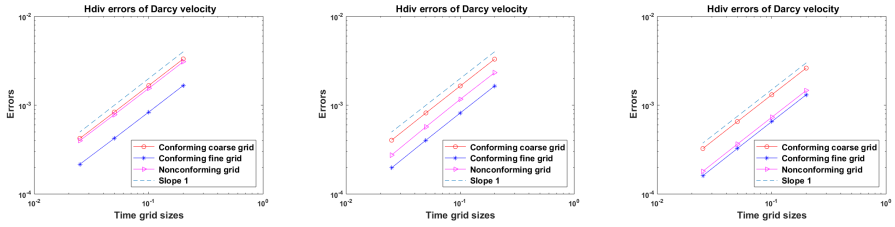

(a) $\alpha_p = 10$ (b) $\alpha_p = 25$ (c) $\alpha_p = 50$

Figure 7: H^{div} errors of Darcy velocity at T = 0.2 by Taylor-Hood elements using $\alpha_f = 0.001$ for different values of α_p.

and right boundaries of the Stokes's domain, and the initial Stokes velocity and the initial Darcy pressure are set to zero. The model parameters are selected as: $\nu_f = 1$, $\nu_p = 50$, $s_0 = 1$, $\alpha = 1$. The Robin parameters are chosen as $\alpha_f = 0.1$ and $\alpha_p = 50$, and the final time is set as $T = 1$. For this test, the Stokes and Darcy equations are approximated using MINI elements and RT1-P1 elements, respectively. To verify the convergence with respect to time with nonconforming time grids, we first compute the reference solution on the mesh size $h = 1/64$ and $\Delta t_{\text{ref}} = 0.01$ and calculate errors using the reference solution. The nonconforming time grids are chosen as $\Delta t_f = \Delta t_p/2$. Table 5 shows errors and convergence rates at $T = 1$ with the fixed mesh size $h = 1/64$, where first order convergence by nonconforming time grids is observed. In Table 6 and Table 7, we compare the accuracy in time of the conforming and nonconforming time grids. In particular, the errors (by nonconforming time grids) in the fluid

domain are close to those by fine conforming time grids, while errors in the porous medium are close to those by coarse conforming time grids.

The velocity magnitude at $T = 1$ using $\Delta t_f = 1/16$ and $\Delta t_p = 1/8$ is shown in Figure 8. As defined in Section 2, $\nu_p \mathbf{I} = \nu_{\text{eff}} \mathbf{K}^{-1}$, where $\mathbf{K}$ is the permeability tensor of the porous medium. For some porous medium like clayey soil or clay the value of coefficients of permeability is around $10^{-5} - 10^{-4}$ meter per day; and about $10^{-8} - 10^{-2}$ meter per day for different kinds of sands [4, 41]. In Figure 9, we show the velocity magnitude at the final time for the porous medium with coefficients of permeability 10^{-5} assuming ν_{eff} to be unity.

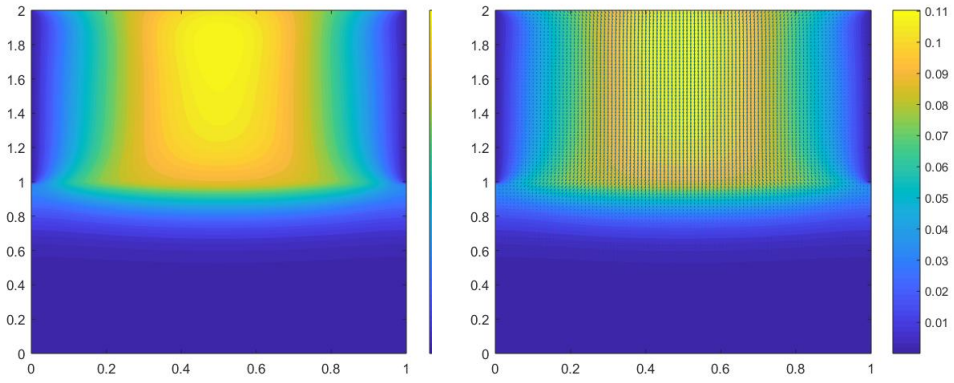

Figure 8: [Test case 2] Velocity magnitude and velocity vector at T = 1 for $\nu_p = 50$.

6. Conclusion

We investigated a space-time DD method based on Robin transmission conditions for the non-stationary Stokes-Darcy system, where the time-dependent local problems are solved independently using local time-stepping schemes with nonconforming time grids. This approach can easily handle problems with discontinuous media represented by model equations with discontinuous coefficients. Also, problems with a large difference in local time scales, e.g., low

Time steps		$\mathbf{u}_f$	p_f	$\mathbf{u}_p$	p_p
Δt_f	Δt_p	H^1 error	L^2 error	H^{div} error	L^2 error
1/4	1/2	2.61e-02	3.58e-02	6.31e-02	2.36e-02
1/8	1/4	1.49e-02 [0.81]	1.52e-02 [1.23]	3.42e-02 [0.88]	1.22e-02 [0.95]
1/16	1/8	7.59e-03 [0.97]	6.48e-03 [1.24]	1.66e-02 [1.04]	6.00e-03 [1.03]
1/32	1/16	3.38e-03 [1.16]	2.67e-03 [1.27]	7.46e-03 [1.15]	2.71e-03 [1.14]

Table 5: : Errors at $T = 1$ using $h = 1/64$ and $(\alpha_f, \alpha_p) = (0.1, 0.5)$.

Time grids	Δt_f	Δt_p	$\mathbf{u}_f$		p_f
			L^2 error	H^1 error	L^2 error
Conforming coarse	1/8	1/8	3.63e-03	1.23e-02	7.98e-03
Nonconforming	1/16	1/8	2.23e-03	7.59e-03	6.48e-03
Conforming fine	1/16	1/16	1.89e-03	6.45e-03	3.18e-03

Table 6: : Errors for the Stokes problem at $T = 1$ using $h = 1/64$ and $(\alpha_f, \alpha_p) = (0.1, 0.5)$.

Time grids	Δt_f	Δt_p	$\mathbf{u}_p$		p_p
			L^2 error	H^{div} error	L^2 error
Conforming coarse	1/8	1/8	1.07e-03	1.84e-02	6.73e-03
Nonconforming	1/16	1/8	9.87e-04	1.66e-02	6.00e-03
Conforming fine	1/16	1/16	5.24e-04	8.82e-03	3.09e-03

Table 7: : Errors for the Darcy problem at $T = 1$ using $h = 1/64$ and $(\alpha_f, \alpha_p) = (0.1, 0.5)$.

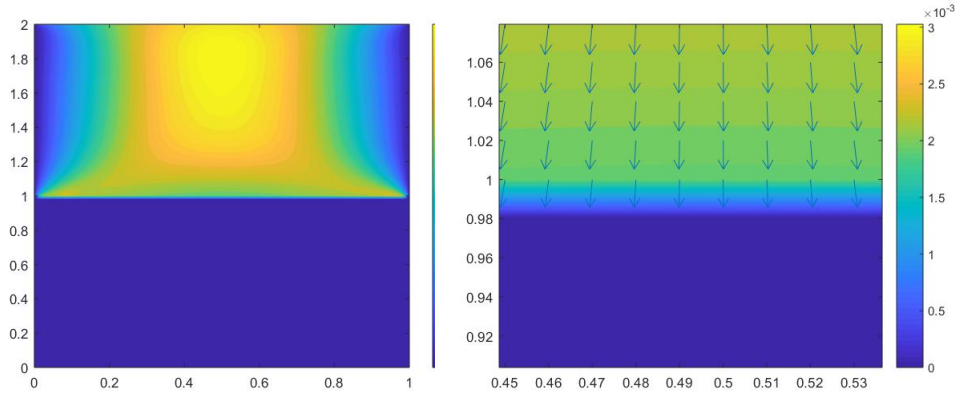

Figure 9: [Test case 2] Velocity magnitude and velocity vector near interface at T = 1 for $\nu_p = 10^5$.

permeability in the Darcy region, can be efficiently solved by the method under discussion. In our numerical tests, we compared errors by conforming and nonconforming time grids, respectively, and observed that using nonconforming time grids significantly improves the efficiency, still yielding the desired accuracy. The robustness of this global-in-time DD approach was also partially verified while being tested on the test case of low permeability porous medium (Figure 9). However, it was noticed that the Darcy velocity among all variables is most sensitive to a choice of Robin parameters for its accuracy. As mentioned earlier, a theoretical framework for the optimal choice of Robin parameters in the SWR method has not been established for time-dependent multiphysics problems; therefore, the parameters used for the presented numerical results were chosen completely based on numerical experiments. For the method to be practical and more robust, further studies are needed for Robin transmission conditions pertaining to the convergence of iterative schemes and the accuracy of numerical solutions. In future work, we plan to extend this approach to other fluid-structure configurations, e.g., the coupled Stokes-Biot system for flows interacting with a poroelastic structure.

References

[1] T. Arbogast and D.S. Brunson, A computational method for approximating a Darcy–Stokes system governing a vuggy porous medium, *Comput.Geosci.* **11**, 2007, pp. 207-218.

[2] T. Arbogast and M. Gomez, A discretization and multi grid solver for a Darcy–Stokes system governing a vuggy porous medium, *Comput.Geosci.* **13**, 2009, pp. 331-348.

[3] I. Babuska and G.N. Gatica. A residual-based a posteriori error estimator for the Stokes-Darcy coupled problem, *SIAM J. Numer. Anal.* **48**, 2010, pp. 498-523.

[4] J. Bear, *Dynamics of fluids in porous media*, Dover Publications, New York, 1988.

[5] D. Bennequin, M.J. Gander and L. Halpern, A homographic best approximation problem with application to optimized Schwarz waveform relaxation, *Math. Comput.* **78**, 2009, pp. 185-223.

[6] C. Bernardi, T.C. Rebollo, F. Hecht and Z. Mghazli, Mortar finite element discretization of a model coupling Darcy and Stokes equations, *Math. Model. Numer. Anal* **42**, 2008, pp. 375-410.

[7] E. Blayo, L. Debreu and F. Lemarie, Toward an optimized global-in-time Schwarz algorithm for diffusion equations with discontinuous and spatially variable coefficients, Part 1: The constant coefficients cas, *Trans. Numer. Anal.* **40**, 2013, pp. 170-286.

[8] Y. Boubendir and S. Tlupova, Stokes-Darcy boundary integral solutions using preconditioners, *J. Comput. Phys.* **228**, 2009, pp. 8627-8641.

[9] M. Cai, M. Mu, and J. Xu, Numerical solution to a mixed Navier–Stokes/Darcy model by the two-grid approach, *SIAM J. Numer. Anal.* **47**, 2009, pp. 3325-3338.

[10] Y. Cao, M. Gunzburger, X. He and X. Wang, Robin–Robin domain decomposition methods for the steady-state Stokes–Darcy system with the Beavers–Joseph interface condition, *Numer. Math.* **117**, 2011, pp. 601-629.

[11] Y. Cao, M. Gunzburger, X. He and X. Wang, Parallel, non-iterative, multi-physics domain decomposition methods for time-dependent Stokes-Darcy systems, *Math. Comput.* **83**, 2014, pp. 1617-1644.

[12] A. Cesmelioglu, V. Girault and B. Rivière, Time-dependent coupling of Navier-Stokes and Darcy flows, *ESAIM: M2AN* **47**, 2013, pp. 539-554.

[13] A. Cesmelioglu and B. Riviere, Analysis of time-dependent Navier-Stokes flow coupled with Darcy flow, *J.Numer. Math.* **16**, 2008,pp. 249-280.

[14] A. Cesmelioglu and B. Riviere, Primal discontinuous Galerkin methods for time dependent coupled surface and subsurface flow, *J. Sci. Comput.* **40**, 2009, pp. 115-140.

[15] W. Chen, M. Gunzburger, F. Hua and X. Wang, A parallel Robin-Robin domain decomposition method for the Stokes-Darcy system, *SIAM J. Numer. Anal.*, **49**, 2011, pp. 1064-1084.

[16] M.M. Dehkordi, A fully coupled porous media and channels flow approach for simulation of blood and bile flow through the liver lobules, *Comput. Methods Biomech. Biomed. Engin.*, **22**, 2019, pp. 901-915.

[17] M. Discacciati, Domain decomposition methods for the coupling of surface and ground- waterflows, PhD dissertation, Ecole Polytechnique Federale de Lausanne, 2004.

[18] M. Discacciati and L. Gerardo-Giorda, Optimized Schwarz methods for the Stokes–Darcy coupling, *IMA J. Numer. Anal.* **38**, 2018, pp. 1959-1983.

[19] M. Discacciati, E. Miglio and A. Quarteroni, Mathematical and numerical models for coupling surface and groundwater flows, *Appl. Numer. Math.* **43**, 2002, pp. 57-74.

[20] M. Discacciati, A. Quarteroni and A. Valli, Robin-Robin domain decomposition methods for the Stokes–Darcy coupling, *SIAM J. Numer. Anal.* **45**, 2007, pp. 1246-1268.

[21] V. Dolean, M. Gander and L. Gerardo-Giorda, Optimized Schwarz methods for Maxwell's equations, *SIAM J. Sci. Comput.* **31**, 2009, pp. 2193-2213.

[22] V. Dolean and F. Nataf, An Optimized Schwarz algorithm for the compressible Euler equations, in Domain Decomposition Methods in Science and Engineering XVI, O. Widlund and D.Keyes (Eds.), Springer, Berlin and Heidelberg, 2007, pp 173-180.

[23] V.J. Ervin, E.W. Jenkins and H. Lee, Approximation of the Stokes-Darcy system by optimization, *J. Sci. Comput.* **59**, 2014, pp. 775-794.

[24] V.J. Ervin, E.W. Jenkins and S. Sun, Coupled generalized nonlinear Stokes flow with flow through a porous medium, *SIAM J. Numer. Anal.* **47**, 2009, pp. 929-952.

[25] J.A. Fiordilino, On pressure estimates for the Navier-Stokes equations, ArXiv e-prints, https://arxiv.org/abs/1803.04366, 2018.

[26] J. Galvis and M. Sarkis, Non-matching mortar discretization analysis for the coupling Stokes-Darcy equations, *Trans. Numer. Anal.* **26**, 2007, pp. 350-384.

[27] J. Galvis and M. Sarkis, FETI and BDD preconditioners for Stokes-Mortar-Darcy systems, *Comm. App. Math. Comp. Sci.* **5**, 2010, pp. 1-30.

[28] M.J. Gander and L. Halpern, Optimized Schwarz waveform relaxation methods for advection reaction diffusion problems, *SIAM J. Numer. Anal.* **45**, 2007, pp. 666-697.

[29] M.J. Gander, L. Halpern and F. Nataf, Optimal convergence for overlapping and nonoverlapping Schwarz waveform relaxation, in The 11th International Conference on Domain Decomposition Methods, C.-H. Lai, P.

Bjørstad, M. Cross and O. Widlund (Eds.), Domain Decomposition Press, Bergen, Norway, 1999, pp. 27-36.

[30] M.J. Gander, L. Halpern and F. Nataf, Optimal Schwarz waveform relaxation for the one dimensional wave equation, *SIAM J. Numer. Anal.* **41**, 2003, pp. 1643-1681.

[31] M.J. Gander and T. Vanzan, On the derivation of optimized transmission conditions for the Stokes-Darcy coupling. In: Haynes R. et al. (eds) Domain Decomposition Methods in Science and Engineering XXV. DD 2018. Lecture Notes in Computational Science and Engineering, **138**, 2020, Springer, Cham.

[32] B. Ganis, D. Vassilev, C. Wang and I. Yotov, A multiscale flux basis for mortar mixed discretizations of Stokes-Darcy flows, *Comput. Methods Appl. Mech. Engrg.* **313**, 2017, pp. 259-278.

[33] G.N. Gatica, S. Meddahi and R. Oyarzua, A conforming mixed finite element method for the coupling of fluid flow with porous media flow, *IMA J. Numer. Anal.* **29**, 2009, pp. 86-108.

[34] K.J. Gavin, New subgrid artificial viscosity Galerkin methods for the Navier-Stokes equations, *Comput. Methods Appl. Mech. Engrg.* **200**, 2011, pp. 242-250.

[35] M. Gunzburger, X.-M. He, B. Li, On Stokes-Ritz projection and multistep backward differentiation schemes in decoupling the Stokes-Darcy model, *SIAM J. Numer. Anal.* **56**, 2018, pp. 397-427.

[36] N.S. Hanspal, A.N. Waghode, V. Nassehi and R.J. Wakeman, Numerical analysis of coupled Stokes/Darcy flows in industrial filtrations, *Transp. Porous Media* **64**, 2006, pp. 1573-1634.

[37] T.T.P. Hoang, Space-time domain decomposition for mixed formulations of heterogeneous problems, PhD thesis, University of Pierre and Marie Currie, Paris. 2013.

[38] T.T.P. Hoang, J. Jaffre, C. Japhet, M. Kern and J.E. Roberts, Space-time domain decomposition methods for diffusion problems in mixed formulations, *SIAM J. Numer.Anal.* **51**, 2013, pp. 3532-3559.

[39] T.T.P. Hoang and H. Lee, A global-in-time domain decomposition method for the coupled nonlinear Stokes and Darcy flows, *J. Sci. Comput.* **87** (22), 2021, https://doi.org/10.1007/s10915-021-01422-1.

[40] W. Jager and A. Mikelic, On the interface boundary condition of Beaver, Joseph and Saffman, *SIAM J. Appl. Math.* **60**, 2000, pp. 1111-1127.

[41] M. Kubacki and M. Moraiti, Analysis of a second-order, unconditionally stable, partitioned method for the evolutionary Stokes-Darcy model, *Int. J. Numer. Anal. Model.* **12**, 2015, pp. 704–730.

[42] W.J. Layton, F. Schieweck and I. Yotov, Coupling fluid flow with porous media flow, *SIAM J. Numer. Anal.* **40**, 2003, pp. 2195-2218.

[43] W. Layton, H. Tran, C. Trenchea, Analysis of long time stability and errors of two partitioned methods for uncoupling evolutionary groundwater-surface water flows, *SIAM J. Numer. Anal.* **51**, 2013, pp. 248-272.

[44] V. Martin, An optimized Schwarz waveform relaxation method for the unsteady convection diffusion equation in two dimensions, *Appl. Numer. Math.* **52**, 2005, pp. 401-428.

[45] M. Mu and J. Xu, A two-grid method of a mixed Stokes-Darcy model for coupling fluid flow with porous media flow, *SIAM J. Numer. Anal.* **45**, 2007, pp. 1801-1813.

[46] M. Mu and X. Zhu, Decoupled schemes for a non-stationary mixed Stokes-Darcy model, *Math. Comput.* **79**, 2010, pp. 707-73.

[47] C. Qiu, X.-M. He, J. Li, and Y. Lin, A domain decomposition method for the time-dependent Navier-Stokes-Darcy model with Beavers-Joseph

interface condition and defective boundary condition, *J. Comput. Phys.* **411**, 2020, https://doi.org/10.1016/j.jcp.2020.109400.

[48] J.R. Ramirez, Time-dependent Stokes-Darcy flow with deposition, PhD dissertation, Clemson University. 2017.

[49] K. Rife and H. Lee, Least squares approach for the time-dependent nonlinear Stokes-Darcy system, *Comput. Math. Appl.* **67**, 2014, pp. 1806-1815.

[50] B. Riviere, Analysis of a discontinuous finite element method for the coupled Stokes and Darcy problems, *J. Sci. Comput.* **22**, 2005, pp. 479-500.

[51] B. Riviere and I. Yotov, Locally conservative coupling of Stokes and Darcy flows, *SIAM J. Numer. Anal.* **42**, 2005, pp. 1959-1977.

[52] I. Rybak and J. Magiera, A multiple-time-step technique for coupled free flow and porous medium system, *J. Comput. Phys.* **272**, 2014, pp. 327-342.

[53] L. Shan, H. Zheng and W.J. Layton, A decoupling method with different sub-domain time steps for the nonstationary Stokes-Darcy model, *Numer. Methods Partial Differ. Equ.* **29**, 2013, pp. 549-583.

[54] S. Tlupova and R. Cortez, Boundary integral solutions of coupled Stokes and Darcy flows, *J. Comput. Phys.* **228**, 2009, pp. 158-179.